



UNIVERSITY OF LEEDS

This is a repository copy of *Megabenthos habitats influenced by nearby hydrothermal activity on the Sandwich Plate, Southern Ocean*.

White Rose Research Online URL for this paper:

<https://eprints.whiterose.ac.uk/184549/>

Version: Accepted Version

Article:

Linse, K, Römer, M, Little, CTS orcid.org/0000-0002-1917-4460 et al. (2 more authors) (2022) Megabenthos habitats influenced by nearby hydrothermal activity on the Sandwich Plate, Southern Ocean. *Deep-Sea Research Part II: Topical Studies in Oceanography*, 198. 105075. ISSN 0967-0645

<https://doi.org/10.1016/j.dsr2.2022.105075>

© 2022 Elsevier Ltd. All rights reserved. This manuscript version is made available under the CC-BY-NC-ND 4.0 license <https://creativecommons.org/licenses/by-nc-nd/4.0/>.

Reuse

This article is distributed under the terms of the Creative Commons Attribution-NonCommercial-NoDerivs (CC BY-NC-ND) licence. This licence only allows you to download this work and share it with others as long as you credit the authors, but you can't change the article in any way or use it commercially. More information and the full terms of the licence here: <https://creativecommons.org/licenses/>

Takedown

If you consider content in White Rose Research Online to be in breach of UK law, please notify us by emailing eprints@whiterose.ac.uk including the URL of the record and the reason for the withdrawal request.



eprints@whiterose.ac.uk
<https://eprints.whiterose.ac.uk/>

1 Megabenthos habitats influenced by nearby hydrothermal activity on the Sandwich Plate, Southern
2 Ocean

3

4 Authors

5 Katrin Linse^{a,*}, Miriam Römer^b, Crispin T.S. Little^{c,d}, Yann Marcon^b, Gerhard Bohrmann^b

6 ^aBritish Antarctic Survey, High Cross, Madingley Road, Cambridge, CB3 0ET, UK

7 ^bMARUM – Center for Marine Environmental Sciences, Department of Geosciences, University of
8 Bremen, Klagenfurter Str, 28359 Bremen, Germany

9 ^cSchool of Earth and Environment, University of Leeds, Leeds, LS2 9JT, UK

10 ^dLife Sciences Department, Natural History Museum, London, SW7 5BD, UK

11 *Corresponding author: kl@bas.ac.uk

12

13 ORCID IDs

14 Katrin Linse 0000-0003-3477-3047

15 Miriam Römer 0000-0003-2540-9286

16 Crispin T.S. Little 0000-0002-1917-4460

17 Yann Marcon 0000-0002-1686-8045

18 Gerhard Bohrmann 0000-0001-9976-4948

19

20 Keywords

21 Abyssal lobsterette, bathyal octocoral assemblages, chimney structure, OFOBS, MTL miniaturized
22 temperature data-logger, micro-bathymetry

23

24 Highlights

- 25 • Unknown areas of hydrothermal activity detected by locally raised temperature
- 26 • Local-scale bathymetric mapping of hydrothermal active sites
- 27 • Presence of chimney structures and bacterial mats at Quest Caldera
- 28 • Megabenthic epifauna comprising known Southern Ocean elements

29

30 Abstract

31 The Sandwich Plate is known as one of the tectonically most active regions in the Southern Ocean and
32 Antarctica, characterised by a subsurface chain of active volcanic islands (the South Sandwich Arc),
33 submarine volcanic features, an earthquake rich area along the South Sandwich Trench and
34 hydrothermal vents on segments of the East Scotia Ridge. In 2013 and 2019 we investigated eight
35 potential hydrothermally active sites in the forearc, island arc and back arc of the Sandwich Plate from

36 shallow (60 m) to abyssal (3886 m) depths. All Protector Seamounts sites, Protector Shoal, Quest
37 Caldera, and an unnamed submarine volcano, showed thermal anomalies, as did the East Scotia Ridge
38 segment E5 back arc site. At Quest Caldera, chimney structures, bacterial mats and mineral
39 precipitates were observed in a depression on the caldera rim. The investigated forearc sites showed
40 hydroacoustic, but not temperature anomalies. None of the sites showed evidence of megafauna
41 associated with hydrothermal venting or hydrocarbon seep sites, but did have evidence of both
42 unexpectedly dense and sparse communities of Southern Ocean taxa in the vicinities of the anomalies.
43 Overall, our investigations showed that the benthic habitats and communities of the Sandwich Plate
44 are still barely known.

45 1. Introduction

46 Discoveries of hydrothermal activity in the waters around Antarctica and confined by the Polar Front
47 (defined as Southern Ocean in Talley et al., 2011), have been made along Antarctic mid-ocean ridges
48 and back-arc spreading centres since the early 2000s (e.g., German et al., 2000; Rogers and Linse,
49 2014; Hahm et al. 2015; Park et al., 2021), the West Antarctic Rift System (e.g., Bohrmann et al., 1999,
50 Van Wyk der Vries et al., 2017) and the South Sandwich Island arc (e.g., Leat et al. 2000; Cole et al.,
51 2014; Linse et al., 2019). More recently influence of hydrothermal activity in the Southern Ocean has
52 been reported on not only bathyal chemosynthetic ecosystems (Rogers et al., 2012; Linse et al., 2019)
53 but also pelagic ecosystems via massive surface phytoplankton blooms (e.g., Ardyna et al., 2019;
54 Schine et al. 2021). Submarine hydrothermal activity in the Southern Ocean seems to affect the
55 biogeochemical cycling and biological ecosystems more than previously thought and therefore
56 research to discover and investigate these hydrothermal active sites gains increasing importance.

57 An area known for hydrothermal activity is the Sandwich Plate (55° – 60° S, 24° – 30° W), an oceanic
58 microplate of about 180,000 km², surrounded by the Scotia Plate to the west, the Antarctic Plate to
59 the south and the South American Plate to the west (Larter et al., 2003; Leat et al., 2013; 2016). The
60 western boundary is the East Scotia Ridge (ESR), a back-arc spreading ridge, and the eastern boundary
61 the South Sandwich Trench, where the South American Plate is subducting (Leat et al., 2004; 2016).
62 The curved South Sandwich volcanic arc spans, from the north, the Protector Seamounts, through
63 eleven islands, of which seven are volcanically active, to seamounts in the south (Leat et al 2013).
64 Submarine explosive eruptions have been reported from Protector Shoal in 1962 (Gass et al., 1963;
65 Holdgate, 1963) and submarine calderas at Southern Thule (Smellie et al., 1998) and Kemp Caldera
66 (Linse et al., 2019).

67 Since 2012, the South Sandwich Islands and the wider Sandwich Plate are included in the South
68 Georgia and South Sandwich Islands Marine Protected Area (SGSSI-MPA) based on their global
69 importance for abundant and unique marine fauna, including benthic fauna at South Georgia and
70 marine mammal and seabird populations in both areas (Trathan et al., 2014; Hogg et al., 2011, 2016,
71 Clubbe, 2018). The benthic habitats of the South Sandwich Islands region range from the shallow
72 intertidal around the islands to hadal depth in the South Sandwich Trench, down to 8266 m at Meteor
73 Deep (Griffiths & Waller, 2016; Bongiovanni et al. 2021). The benthic diversity for this habitat-diverse
74 region is poorly known and under sampled. The deeper sublittoral (>100 m) and upper bathyal (>1500
75 m) depths have been investigated during the LAMPOS (Arntz et al., 2005a, b), BIOPEARL I (Kaiser et al.
76 2008; Griffith et al. 2009), IceFish (Lockhardt and Jones, 2008) and BlueBelt expeditions (Downie et
77 al., 2021; Hogg et al. 2021). These studies indicated that the South Sandwich Islands combine benthic
78 faunal elements of the Antarctic and sub-Antarctic faunas and there also seemed to be a boundary for
79 distributions of some species within the island arc (Arntz et al., 2004b, Hogg et al., 2021). Knowledge
80 for the deep bathyal, abyssal and hadal depth is based on the Russian deep-sea investigations in the
81 middle of the last century (Malyutina, 2004 and references therein), the Antarctic benthic Deep-Sea
82 Biodiversity Project ANDEEP II expedition in 2002 (Brandt et al. 2004, 2007) and, more recently, the
83 Five Deeps Expedition to the hadal part of the South Sandwich Trench (Stewart and Jamieson, 2019;
84 Jamieson et al. this issue), as well as from the Biogeography of Deep-Water Chemosynthetic
85 Ecosystems in the Southern Ocean (ChEsSO) expeditions, which investigated hydrothermal active
86 habitats specifically (e.g. Rogers et al., 2012; Linse et al., 2019). The three ChEsSO expeditions
87 discovered and investigated hydrothermal vents at the ESR segments E2 and E9, and at the southern
88 island arc sites of the Kemp Caldera and Adventure Crater (Rogers et al. 2012; Tyler, 2011; Linse 2019),
89 and described their megabenthic fauna and communities (e.g., Marsh et al., 2012; Reid et al. 2013;
90 Mah et al., 2015; Thatje et al., 2015).

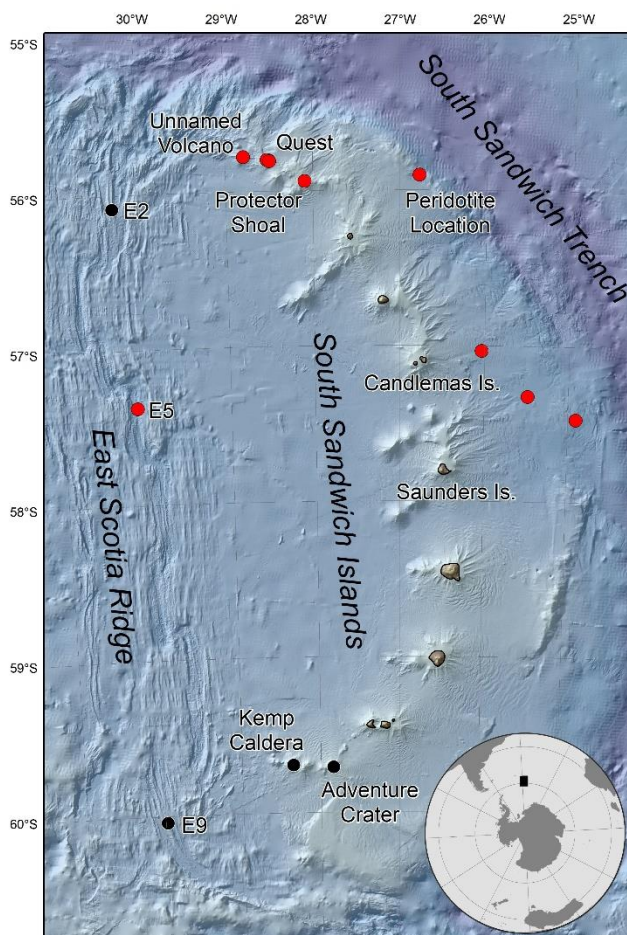
91 The aims of the RV Polarstern expeditions PS81 in 2013 and PS119 in 2019 were to investigate likely
92 sites of hydrothermal activity on the Sandwich Plate, including locations in the back-arc, forearc and
93 at the Protector Seamounts, by in-situ imagery, and to describe the examined habitats and to assess
94 their faunal elements for chemosynthetic and Southern Ocean connections.

95

96 2. Material and Methods

97 2.1. Study Area and expeditions

98 The RV Polarstern expeditions PS81 in 2013 and PS119 in 2019 investigated locations on the Sandwich
99 micro-plate for hydrothermal activity (Bohrmann, 2013; 2019). Particularly in the northern area of the
100 arc, acidic volcanic cones reach up to 400 – 50 m below sea level (Leat et al., 2013; 2016). Based on
101 preliminary results of previous hydroacoustic seafloor and water column surveys indicating potential
102 hydrothermal activities on the microplate (German et al., 2000; Frenzdorff et al., 2002; Leat et al.,
103 2004), eight locations in the northern arc area, the forearc and the ESR segment E5 were investigated
104 (Figure 1).



105

106 Figure 1. Positions of the investigated locations in the vicinity of the South Sandwich Islands on the
107 Sandwich Plate. Inset map shows the position of the South Sandwich Islands in relation to Antarctica.

108 Black dots – known hydrothermal sites, red dots – investigated sites. Bathymetry based on
 109 dx.doi.org/10.5285/b8143952-421c-4544-8437-58f339253d30.

110

111 2.2. Towed camera platform systems

112 During the RV Polarstern expeditions PS81 and PS119, three types of towed camera systems were
 113 deployed to image and survey the deep-sea seafloor (Table 1): OFOS (ocean floor observation system),
 114 OFOBS (ocean floor observation and bathymetry system) and TV-sled.

115 Table 1. Geographic positions of camera deployments in the vicinity of the South Sandwich Islands on
 116 the Sandwich Plate. MAPR – miniature autonomous plume recorder; MTL – miniaturized temperature
 117 data-logger

118

Area Location	Station	Date	Gear	Latitude (S)		Longitude (W)		Depth (m)		Attachments
				Start	End	Start	End	Start	End	
Protector Seamounts										
Quest Caldera	PS81/268-1	31.03.2013	OFOS	55°48.219	55°48.724	28°30.144	28°30.029	731	744	4 MTLs
	PS81/268-2	31.03.2013	OFOS	55°48.008	55°49.366	28°31.488	28°32.136	731	950	4 MTLs
	PS81/276-1	08.04.2013	TV-sled	55°48.542	55°48.652	28°29.687	28°29.516	716	717	5 MTLs
Protector Shoal	PS81/275-1	08.04.2013	TV-sled	55°56.426	55°57.097	28°05.728	28°06.693	60	526	5 MTLs
Unnamed volcano	PS81/278-1	09.04.2013	TV-sled	55°46.711	55°46.873	28°47.601	28°47.459	618	779	5 MTLs
Forearc										
off Saunders Island I	PS81/270-1	02.04.2013	OFOS	57°28.190	57°28.285	24°54.174	24°55.174	3659	3681	2 MTLs*
off Saunders Island II	PS81/274-3	08.04.2015	TV-sled	57°19.605	57°19.536	25°29.072	25°29.178	3723	3725	3 MTLs
off Candlemas Island	PS81/273-1	07.04.2013	TV-sled	57°02.028	57°02.063	26°02.221	26°02.225	3025	3026	3 MTLs*
Peridotite Location	PS119/046-1	16.05.2019	OFOBS	55°54.159	55°54.429	26°46.530	26°47.041	2500	2313	3 MTLs, MAPR
East Scotia Ridge										
Segment E5	PS119/032-1	10.05.2019	OFOBS	57°22.567	57°27.705	30°07.266	30°07.326	3886	3649	3 MTLs, MAPR
* no data acquisition										

119

120

121 2.2.1. OFOS

122 During PS81 in 2013, the Alfred Wegener Institute (AWI) towed underwater camera system OFOS with
 123 a high-resolution digital camera (iSiTEC, CANON EOS 1Ds Mark III) was used. The three main
 124 components are a deck unit, a single-mode-optical fiber cable and an underwater unit. The
 125 underwater unit is mounted in a steel frame with dimensions of 140L X 92W X135H cm. The camera,
 126 two flashlights (iSiTEC UW-Blitz 250, TTL driven), three red laser pointers (Oktopus, Germany) at 50
 127 cm to each other, four LED lights and a Tritech Altimeter are attached to the frame. The camera
 128 footprint at 1.5 m above seafloor encompasses 3–4 m². The deployment is controlled by the deck unit
 129 and five different software modules installed on a laptop computer control the operation of the
 130 components and save the images and positions.

131 The OFOS was deployed from the side of the Polarstern and towed at a speed of ~0.5 – 0.7 knots at a
 132 minimum distance of 1.5 m above the seafloor. The target altitude of 1.5 m varied considerably as a
 133 winch operator manually adjusted the cable length and adapted to varying bottom topography and
 134 sea state and ranged from 1.4 m to 15 m above the seafloor. If the distance to the seafloor is too far,
 135 the laser pointers are not visible on the image and only images below an altimeter depth of 10 m were
 136 analysed. To determine the position of the OFOS and to locate the positions of the images taken, a
 137 ship’s ultra-short baseline system (USBL) Posidonia transponder was fixed to the frame of the OFOS.

138

139 2.2.2. TV-sled

140 The MARUM TV-sled was used during PS81 when technical problems did not allow for OFOS
141 deployments. The TV-sled is a towed camera system transmitting an analogue video signal from the
142 sled through the ship's coax cable to the deck unit. The main components are the video-data telemetry
143 system consisting of a deck unit and an underwater system with a black-and-white camera system and
144 a high intensity discharge light. The black-and-white video signal transmitted by the video-data-
145 telemetry system is displayed in real time on monitors and recorded by a VCR.

146 The underwater system is mounted in a steel frame with dimensions of 120L x 80W x 120H cm. The
147 sled was also towed at a speed of 0.5 to 1 knots at a distance of about 3 m above the ground. This
148 distance is maintained by a winch operator manually adjusting the cable length, such that a weight
149 suspended 3 m below the sled is flying just above the seafloor. The length of the weight is ~25 cm and
150 can be used for size estimation on the seafloor when visible in the image. A USBL Posidonia
151 transponder was attached to the frame during deployment for underwater positioning.

152

153 2.2.3. OFOBS

154 During PS119 in 2019, the AWI ocean floor observation and bathymetry system (OFOBS) was used for
155 visual inspection (Purser et al., 2019). The system is deployed with a continuous direct communication
156 through the ship's fiber optic cable and operational at depths up to 6,000 m. The OFOBS frame is
157 equipped with a deep-sea underwater telemetry system including 4 LED lamps, 2 flashes, 3 laser
158 pointers, a high-resolution digital camera (iSiTEC, CANON EOS 5D Mark III) for still pictures and a HD
159 colour video camera (Sony FCB-H11). A USBL Posidonia transponder and a Trittech altimeter are
160 mounted for underwater positioning and depth control. However, the altimeter did not function
161 during the dive of station PS119/032-1, therefore, a safe distance to the seafloor was maintained
162 suitable for the 3-dimensional topography of the site. At station PS119/046-1 the altimeter range for
163 images varied between 4 m and 14.1 m. If the distance to the seafloor was too far away, the laser
164 pointers were not visible on the image.

165

166 2.2.4. Additional sensors

167 Miniaturized temperature data-logger (MTL, Pfender and Vilinger, 2002), autonomous high-precision
168 thermometers for deep-sea application rated to 6000 m depth, were connected to the camera system
169 frames to measure near-seafloor temperatures along the survey paths. Their accuracy is within the
170 range of 5 – 1 mK, depending on the temperature range and precision up to 1 mK. Between two and
171 five MTLs were mounted on OFOS, OFOBS and TV-sled and sampled bottom water temperatures at a
172 1 Hz frequency during all dives. Mounted diagonally across the bottom and top of the frames they
173 successfully registered bottom water anomalies.

174 A miniature autonomous plume recorder (MAPR; Walker et al. 2007), built by the Pacific Marine
175 Environmental Laboratory (PMEL), Seattle, was connected to the OFOBS deployed during the PS119
176 cruise in 2019. The MAPR contains the following probes: 1) a pressure gauge with a range of 0-400
177 bars to record the water depth; 2) a thermistor with a resolution of 0.001°C mounted in a titanium
178 probe; 3) a light back scattering sensor (LBSS, or "nephelometer") that senses scattered light from a
179 small volume within centimetres of the sensor window; and 4) an oxidation-reduction potential (ORP)
180 sensor that responds to reduced hydrothermal chemicals in the water column. ORP detects
181 hydrothermal discharge of all temperatures, including low-temperature diffuse venting as well as
182 higher-temperature but particle-poor sources. It responds immediately, with decreasing potential

183 values (E(mV)), to the presence of nanomolar concentrations of reduced hydrothermal chemicals such
184 as Fe⁺², HS⁻, H₂ that are out of equilibrium with the oxidizing ocean (Walker et al., 2007). These
185 chemicals rapidly oxidize or metabolize near their seafloor source.

186

187 2.3. *Hydro-acoustic data*

188 Multibeam surveys were conducted by the RV Polarstern's hull-mounted multibeam echo sounder
189 systems, HYDROSWEEP DS3 (Teledyne RESON, formerly ATLAS) with water-column imaging capability.
190 The multibeam echosounder had a nominal sounding frequency of 14–17 kHz, which enabled
191 hydroacoustic recording below 30 mbsl down to full ocean depth. The swath width was set in the deep
192 sea to a coverage of 3.5 times and in the shallower areas of 5 times the water depth. Multibeam data
193 were processed using MB-System suite software (Caress & Chayes, 2017) and CARIS Hips & Sips
194 (Teledyne) to produce seafloor bathymetry and backscatter grids with a resolution of 35 - 70 m grid
195 cell size.

196 The hull-mounted single-beam echosounder Parasound P70 (Teledyne RESON, formerly ATLAS) is
197 capable to act as a sub-bottom profiler and for water column investigations. The opening angle of the
198 transducer array is 4° by 5°, which corresponds to a footprint size of about 7% of the water depth. The
199 device utilizes the parametric effect based on the nonlinear relation of pressure and density during
200 sonar propagation (Spiess and Breitzke, 1990). The primary high frequency (~19 kHz) allows imaging
201 water column anomalies, whereas the secondary low frequency (~4 kHz) is used to image subsurface
202 structures. The acquisition software ATLAS PARASTORE was used to store and display the echograms.

203

204 2.4. Qualitative assessment of megabenthic epifauna and habitats

205 The still images and video footage were assessed to describe the present megabenthic epifauna and
206 seafloor substrate. During each deployment, digital and manual logs were written to document
207 common, as well as rare fauna, and geological structures. Low quality images (too dark, too high
208 altitude, extensive sediment clouds) were omitted from the analyses. To account for camera lens edge
209 distortion effects, the images were split into 100 equal sized rectangles and the outer two rectangle
210 layers were excluded, leaving 36 rectangles for analysis. Still images were analysed to assess
211 percentage cover of abiotic and biotic substrate types following the sedimentary size classification of
212 Tucker, 1991: mud, sand, gravel, pebbles, cobbles, boulders, or bedrock, with the addition of pillow
213 lava and talus to note volcanogenic origin. Megafaunal taxa were counted. In-situ image-derived
214 taxonomic identification to lower taxonomic levels is difficult, especially in low resolution or far-
215 distant images. Additionally, recent molecular studies have shown high numbers of cryptic species
216 complexes in the Antarctic benthic fauna (e.g., Grant and Linse, 2009; Brasier et al., 2016; Riuz et al.
217 2020). Therefore, we followed the recommendations of Horton et al. (2021) for identification of in-
218 situ images. Hence, our identifications were based on established phylum and class levels, in selected
219 compelling taxa family or genus levels. We used 'indet.' to denote an undetermined species, and
220 Rauschert and Arntz (2015) and, if appropriate, taxon specific literature for identifications.

221

222 3. Results

223 3.1. Site descriptions

224 Eight potential hydrothermal active sites on the South Sandwich microplate have been investigated
 225 by still and video imagery during nine towed camera system deployments (Table 2). The sites varied
 226 from volcanic cones at the Protector Seamounts to potential seep sites in the forearc and venting sites
 227 in the back-arc ridge system. At all sites exposed rock, often of obviously volcanogenic origin, was
 228 present, with various amounts of sediment between the rock outcrops. The megabenthic epifauna
 229 observed on the still and video imagery varied in abundance and diversity within and between sites,
 230 independent of depth. Hard substrates served as habitat for suspension feeding taxa, like hard and
 231 soft corals, hydrozoans, bryozoans, crinoids and sponges, whilst ophiuroids and holothurians were
 232 more abundant at sites with more soft sediment.

233 Table 2. Number of images and seafloor temperatures per camera deployments.

234

Area	Station	Imagery	Altimeter	Depth range	Seafloor temperature	
Location		stills/ min VHS	range (m)	(m)	ambient	raised / depth
Protector Seamounts						
Quest Caldera	PS81/268-1	379/-	4.0-9.9	731-744	0.4°C	0.6-0.75°C / ~720 m
	PS81/268-2	499/-	1.3- 9.9	731-950	0.38-0.45°C	-
	PS81/276-1	-/127	-	716-717	0.5°C	0.6-2.7°C / ~716 m
Protector Shoal	PS81/275-1	-/126	-	60-526	0.25-0.4°C	0.6-0.85°C / ~460-520 m
Unnamed volcano	PS81/278-1	-/119	-	618-799	0.5°C	0.8-2°C / ~590-620 m
Forearc						
off Saunders Island I	PS81/270-1	55/-	1.4 - 8.8	3659-3681	nd	nd
off Saunders Island II	PS81/274-3	-/97	-	3723-3725	-0.4°C	-
off Candlemas Island	PS81/273-1	20/-	2.2 - 6.1	3025-3026	nd	nd
Peridotite Location	PS119/046-1	520/-	4 - 14.1	2500-2313	-0.2°C	-
East Scotia Ridge						
Segment E5	PS119/032-1	50/-	-*	3649-3886	0°C	0.5°C / ~3600 m
*altimeter did not function						

235

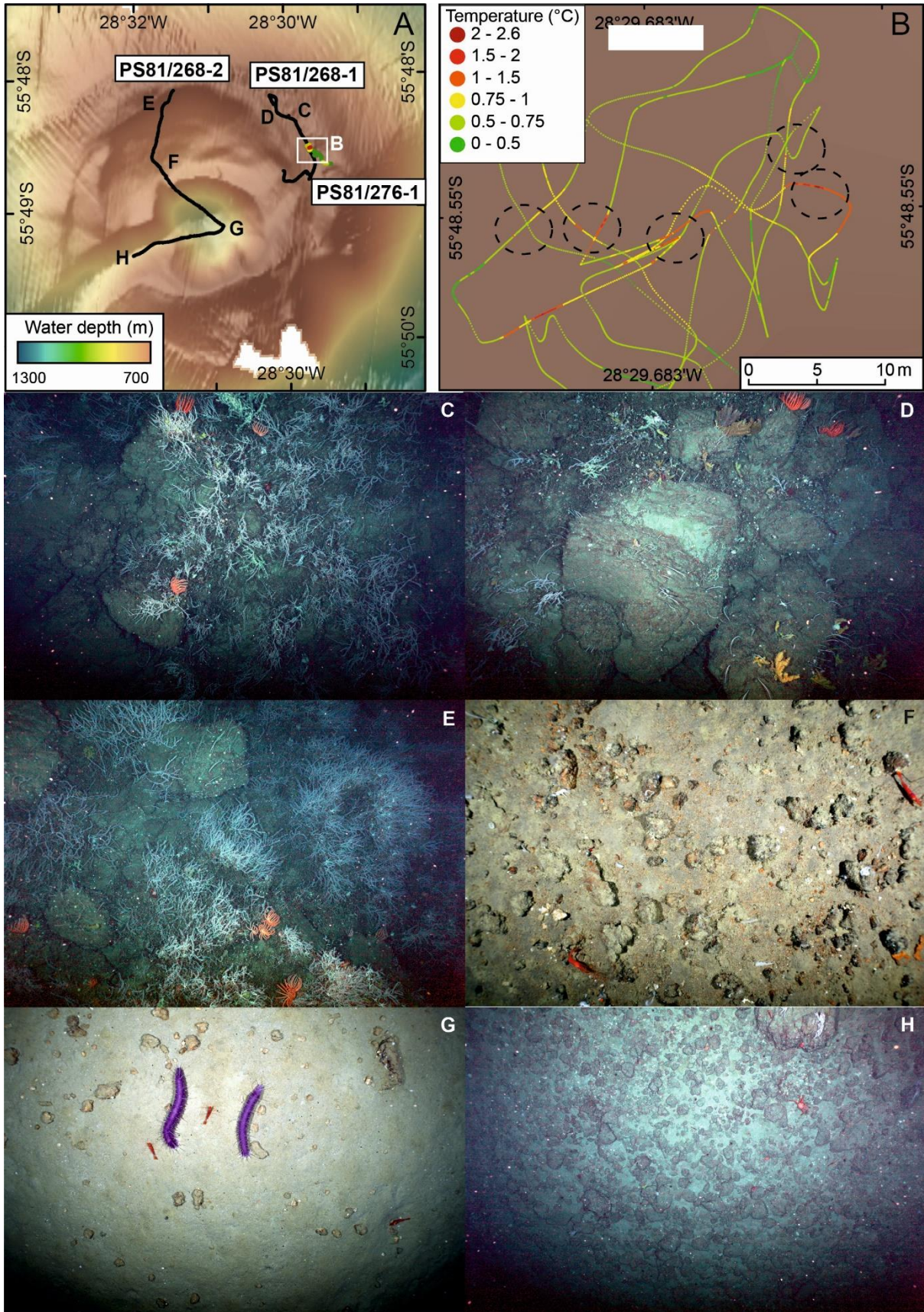
236 3.1.1. Protector Seamounts - Quest Caldera

237 The Quest Caldera, a volcanic structure with an outer and inner caldera, was investigated during 3
 238 camera dives from the outer top and rim of the structure, to the inner caldera and down a chute-like
 239 structure (Table 1,2, Figure 2A). The upper rim of the structure is at about 720 m water depth, while
 240 the central part of the caldera is at 1075 m, about 340 m deeper than the rim. The distance from the
 241 rim to the centre is ~1.8 km. After discovery of thermal anomalies on the north-east rim during dive
 242 PS81/268-1 the site was further investigated during dive PS81/276-1 and chimney structures with
 243 microbial mats and/or whitish precipitates about 1 m in extent were observed in a steep-walled
 244 depression, roughly 10 m deep of about 12 x 24 m across. In this depression, the water temperature
 245 reported by the MTLs on the camera frame was raised 2.7°C above the ambient temperature of 0.5°C
 246 outside the depression (Figure 2B). Neither shimmering water, nor vent-endemic megafauna known
 247 from the East Scotia Ridge vents (e.g., *Kiwa* crabs, stalked barnacles, peltospirid gastropods or
 248 vesicomid clams) were seen.

249 The upper rim of the caldera was covered by volcanic blocks with aged appearance. These had sizes
 250 ranging from several centimetres to few meters and had sediments between them (Figure 2 C-E). A
 251 diversity of suspension-feeding organisms in abundance was observed during the entire deployment,
 252 especially on the elevated blocks. There were scattered areas with many a white, branched octocoral,
 253 which in turn served as habitat for other organisms, such as suspension feeding brittle stars and
 254 sponges. Other common fauna on the volcanic blocks were elongated *Primnoella*-like octocorals,
 255 orange *Thourella*-like bottlebrush octocorals, yellow sponges, bryozoans, yellow stalked crinoids and

256 red brisingid starfish (Figure 2 C-E). Occasional red lithodid spider crabs of the genus *Paralomis* were
257 observed (Figure 2 H), representing a typical sub-Antarctic faunal element, as well as macrourid fish
258 (rattails) and red *Nematocarcinus* shrimps (Figure 2 F-H), which are also found in the Southern Ocean
259 and in deep-sea habitats.

260 The suspension feeding fauna was less abundant on the inner caldera slope of Quest Caldera. On the
261 floor of the first caldera plateau the sediment included colourful gravel near to the slope, which
262 gradually decreased in grain size and volume with increasing distance from the slope (Figure 2 F). The
263 gravel served as attachment sites for a variety of sessile suspension feeding animals, including
264 primnoid and white, branching fan-like isidid octocorals, some sponges, bryozoans and serpulid
265 worms. There were also a few white infaunal anemones and orange epifaunal anemones. Rattails,
266 *Paralomis* and *Nematocarcinus* were present and increased in abundance where the gravel gave way
267 to finer sediments. The wall of the inner caldera was abrupt with a talus slope descending into the
268 inner caldera structure. Only a few animals were observed on the slope. The floor of the inner caldera
269 was like that of the outer caldera plateau, with gravel and finer sedimented areas. The deepest part
270 of the caldera had fewer suspension feeding epifauna, with occasional primnoid octocorals and soft
271 corals, while *Nematocarcinus* was still abundant. Occasionally larger, mobile fauna like rattails and
272 holothurians were seen (Figure 2G). The floor of the chute-like structure that runs south-west from
273 the nested caldera varied from sandy areas with scattered blocks to talus slopes. The blocks were
274 settled by occasional white branched, fan-like octocorals and stalked crinoids; *Paralomis* and
275 *Nematocarcinus* were also present (Figure 2 H).



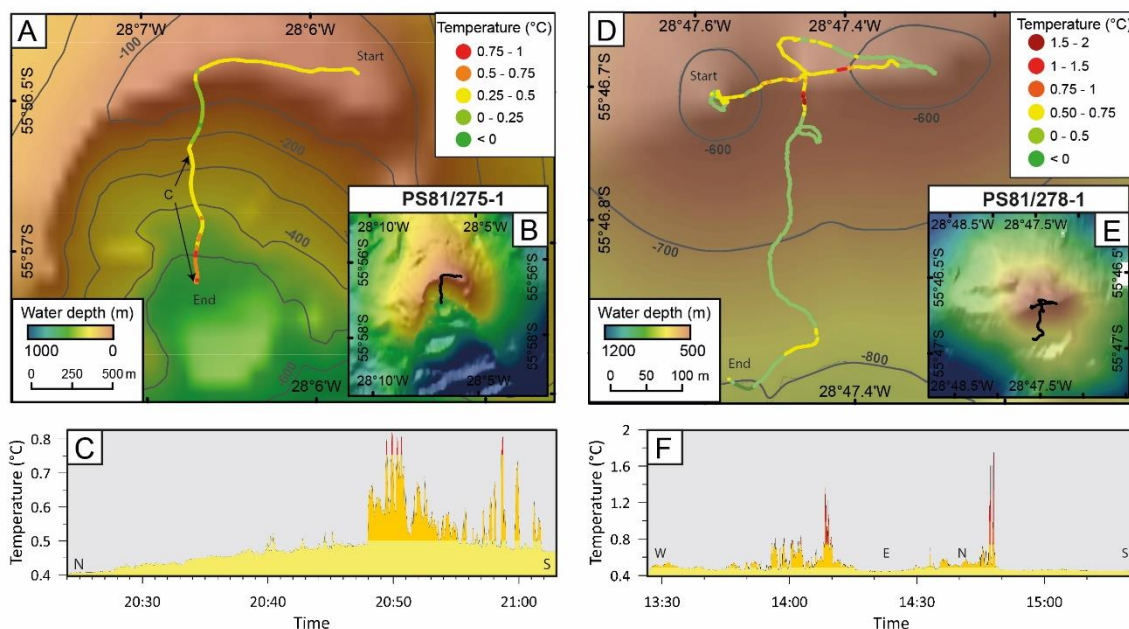
278 Figure 2. Positions of OFOS and TV-sled dives and in-situ habitat images at the Quest Caldera. A) Dive
279 transects of PS81/268-1, PS81/268-2 and PS81/276-1; B) Position of temperature anomalies on the

280 outer rim of the Quest Caldera during PS81/276-1. Observed hydrothermal activity indicators, such as
 281 microbial mats or chimney structures are circled; C) Dense suspension feeding epifauna including soft
 282 corals and brisingid star fish on the top of the caldera 250 m away from hydrothermal anomalies and
 283 chimney structures ; D) Suspension feeding epifauna including soft corals and brisingid star fish on the
 284 outer rim of the caldera 400 m away from hydrothermal anomalies and chimney structures ; E) Dense
 285 suspension feeding epifauna including soft corals and brisingid star fish on the outer rim of the caldera
 286 2500 m away from hydrothermal anomalies and chimney structures ; F) Decapod (*Nematocarcinus*
 287 indet.) and mysid shrimps on the talus slope to the inner caldera rim; G) Decapod shrimps
 288 *Nematocarcinus* indet. and holothurian *Bathylotes* indet. on the soft and gravel sedimented inner
 289 caldera floor; H) Decapod shrimps *Nematocarcinus* indet. and spider crab *Paralomis* indet. on talus
 290 slope of the chute-like structure.

291

292 3.1.2. Protector Seamounds - Protector Shoal

293 Protector Shoal, a shallow, submarine volcano with a collapsed flank, was investigated from its top at
 294 around 60 m depth to 526 m depth at circular depression on the flank (Figure 3A, B). Elevated
 295 temperatures of 0.4-0.6°C above ambient were recorded on the inner slope of the circular depression.
 296 The top of Protector Shoal showed north-south running low ridges, about one metre apart, of pale
 297 coloured lava and within the ridges darker, coarse sediment. Towards the rim the substrate changed
 298 to pitted lava with lava collapse structures, which were densely colonised (~10 per m²) by broad, single
 299 bladed seaweeds, which disappeared below 66 m depth. The slope of the flank deeper than 100 m
 300 consisted of sand, gravel, and isolated lava boulders. Large cidarid urchins were commonly observed
 301 as well as occasional *Paralomis* specimens, anemones and macrourid fish. At 500 m depth the gravel
 302 changed briefly to pitted lava, indicating an area that may correspond to the recorded temperature
 303 anomaly, before continuing to 526 m at the end of dive.



304

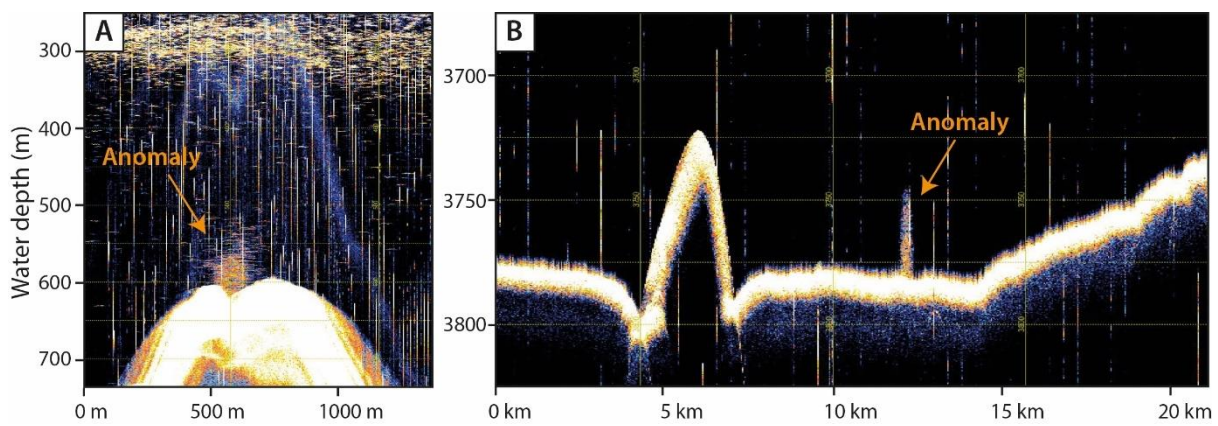
305 Figure 3. Positions of TV-sled at Protector Shoal and an unnamed volcano. A) Dive transect and
 306 temperature anomalies of PS81/275-1 at Protector Shoal; B) Overview map of Protector Shoal; C)
 307 Temperature anomalies along PS81/275-1 dive track; D) Dive transect and temperature anomalies of

308 PS81/278-1 at an unnamed volcano; E) Overview map of the unnamed volcano; F) Temperature
309 anomalies along PS81/275-1 dive track.

310 3.1.3. Protector Seamounts - Unnamed volcano

311 The unnamed volcano (55°46 S 28°47 W, 618 m) was initially investigated by an hydroacoustic survey
312 based on its double-peaked structure, and a high raising plume-like anomaly was detected in the
313 saddle area between the peaks (Figure 3D, E; 4A)). The two peaks and the flanks were formed of gravel
314 and larger volcanic rock outcrops. Numerous lithodid crabs were seen on the gravel on top of the
315 peaks, but no other megabenthos was visible. No fauna was observed on the deeper gravel flanks
316 between the peaks where thermal anomalies of 0.-1.5°C above ambient were recorded (Figure 3F;
317 Table 2). On the flank of the eastern peak large rock outcrops and steep scarp of exposed lava were
318 seen. These were colonised by suspension feeding brisingid starfish, large isidid octocorals and stalked
319 anemones. The outer flank from the saddle deep downwards consisted of talus slopes of initially
320 decimetre-sized rocks and then gravel. Numerous lithodid crabs were observed with more than 10
321 crabs in the field of view. Between 620 m and 750 m depth the gravelly sediment with occasional
322 larger blocks was colonised by large isidid octocorals with more than 50 individuals in the field of view,
323 as well as with primnoid octocorals and brisingid starfish.

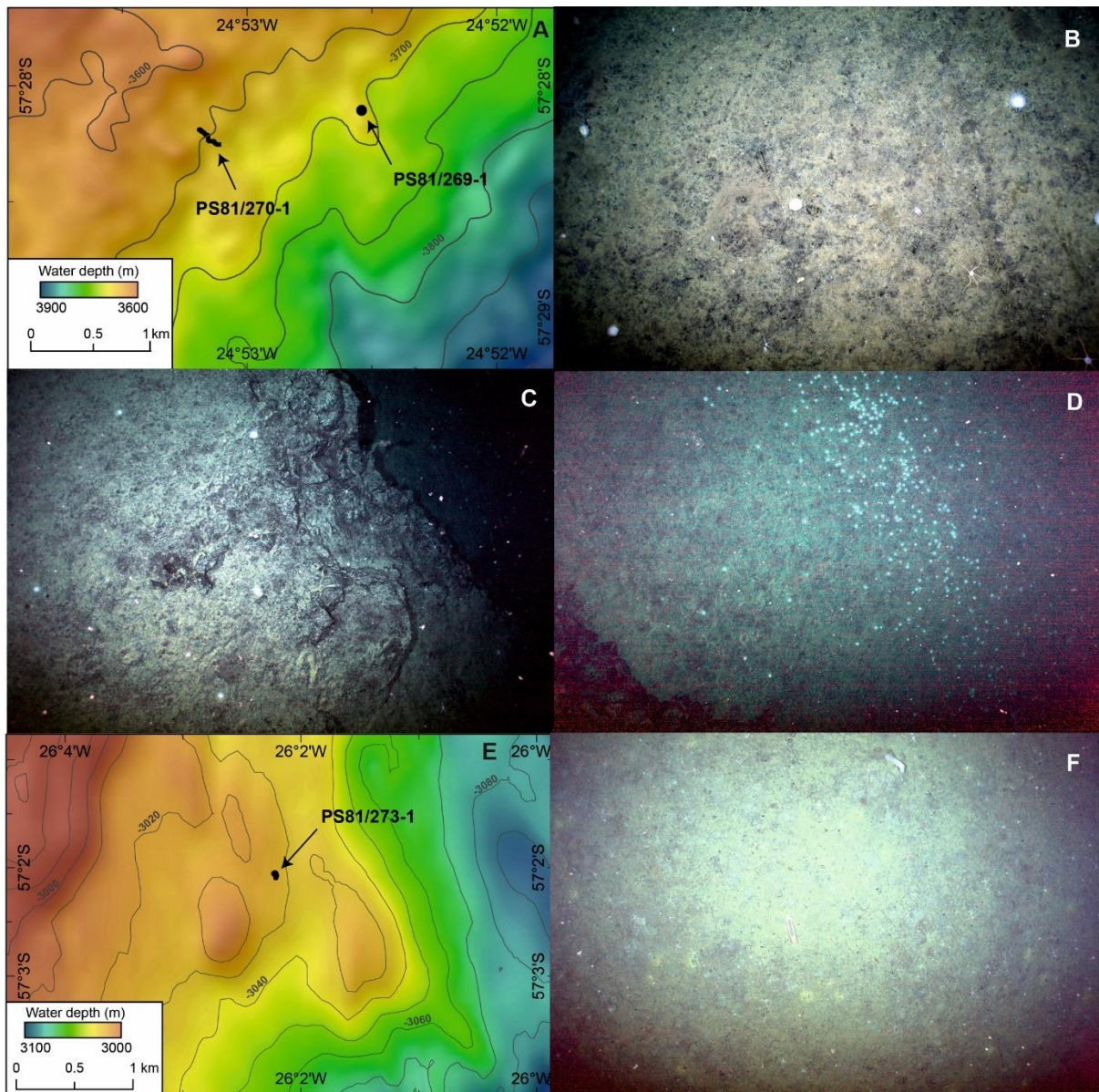
324



325
326 Figure 4. Hydroacoustic anomalies at Protector Seamounts and the Forearc. A) Plume-like, ~ 100 m
327 high, anomaly observed by hydroacoustics in the saddle of the unnamed volcano during PS81/270-1;
328 B) Hydroacoustic anomaly reaching about 35 m from the seafloor off Saunders Island at position of
329 dive PS81/274-3.

330 3.1.4. Forearc – off Saunders Island I

331 The Forearc area off Saunders Island was investigated based on high seafloor backscatter in the
332 HAWAII sidescan sonar map (Vanneste and Larter, 2002) during dive PS81-270-1 (Figure 5A). The
333 northern part of the high-backscatter patch in about 3,660 m depth consisted of a relatively flat
334 seafloor covered by coarser, gravelly sediment showing traces of Lebensspuren, biologically formed
335 structures in sediments, as well as ophiuroids, holothurians and occasional white anemones (Figure
336 5B). Patches of greenish colour indicated sunken phytodetritus serving as food source for epi- and
337 infaunal taxa. Occasional escarpments, or glassy looking and brecciated volcanic rock occurrences
338 were seen (Figure 5C). One scarp was a few meters high and at the bottom a very dense and localised
339 patch of white anemones was observed (Figure 5D). Beyond this area, gravelly sediment with
340 occasional white anemones, ophiuroids and holothurians continued.



341

342 Figure 5. Potential seep areas based on sidescan backscatter anomalies in Forearc. A) Map of
 343 PS81/269-1 and PS81/270-1 tracks off Saunders Island; B) Gravelly sediment with large blocks showing
 344 Lebensspuren and inhabited by white anemones, ophiuroids and red shrimps; C) Escarpment of glassy
 345 looking volcanic rocks; D) Large numbers of white anemones below escarpment; E) Map of PS81/273-
 346 1 track off Candlemas Island; F) Gravelly sediment with large blocks showing Lebensspuren and
 347 inhabited by white anemones, ophiuroids and red shrimps.

348

349 3.1.5. Forearc – off Saunders Island II

350 On the forearc slope off Candlemas Island (57°19 S 25°29 W, 3723 m) a hydroacoustic flare-like
 351 anomaly reaching about 35 m into the water column was detected, and the area was investigated
 352 during OFOS dive PS81/274-3 (Figure 4B). The area was characterised by relatively flat, gravel and finer
 353 sediment covered seafloor and elevated areas with large volcanic blocks, some of which appeared to
 354 have fractured edges. The gravelly sediment areas had abundant Lebensspuren, ophiuroids,
 355 holothurians and occasional macrourid fish.

356

357 3.1.6. Forearc – off Candlemas Island

358 The forearc area off Candlemas Island was investigated based on high seafloor backscatter in the
359 HAWAII sidescan sonar map (Vanneste and Larter, 2002) during dive PS81-273-1 (Figure 5E). No
360 temperature anomalies were observed (Table 2). The seafloor was relatively flat, sediment with
361 occasional gravel and covered in a fine greenish layer of phytodetritus (Figure 5F). Large numbers of
362 epi- and infauna were visible, including several species of ophiuroids and at least three different
363 species of large holothurians: *Bathyploetes* indet., a pale elasipodid and a purple elasipodid. The
364 frame's bow wave occasionally pushed the phytodetritus and top sediment layer off, revealing
365 numerous tubes, probably of polychaete origin.

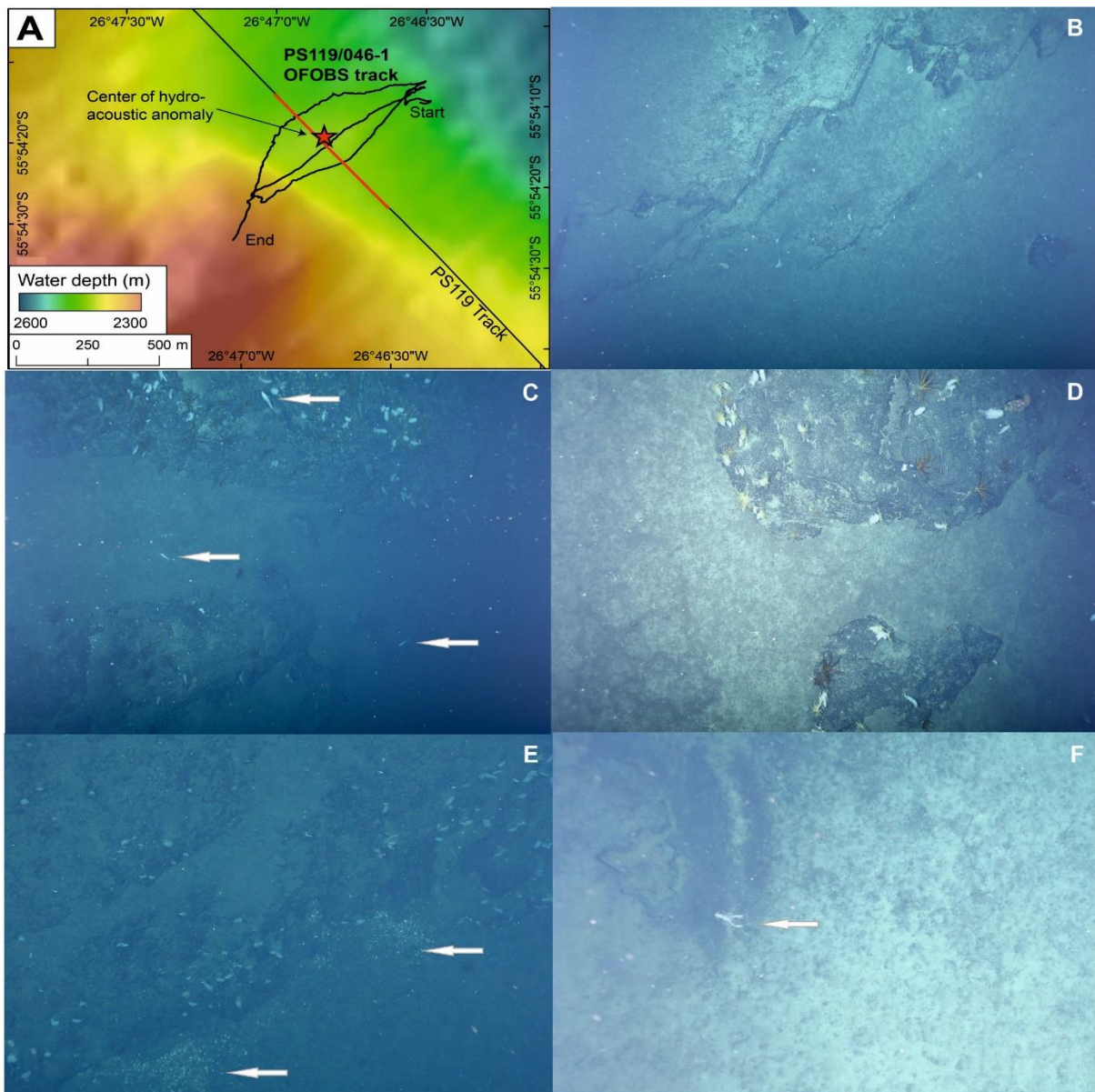
366

367 3.1.7. Forearc - Peridotite Location, off Zavodovski Island

368 Intensely serpentinized peridotites were dredged during a previous British expedition in the fore-arc
369 area off Zavodovski Island (Pearce et al., 2000). This area was selected as a site for investigation
370 because abiogenic methane production is a known product of the serpentinisation process and could
371 be seeping from the seafloor here. During PS81 and PS119, hydroacoustic anomalies were detected
372 at a ridge structure in this location. In 2019 (PS119), a camera dive was conducted across an arc-
373 parallel ridge around the most prominent hydroacoustic water column anomaly (Figure 6A). The
374 seafloor was characterised by volcanic rock outcrops and escarpments, often without sediment cover,
375 and flatter, gravelly sedimented areas. The hard-rock outcrops at bathyal depths of over 2300 m in
376 southern-eastern part of the investigated area were densely colonized by a rich epifaunal suspension
377 feeder assemblage, including comatulid and stalked crinoids, isidid and primnoid octocorals, as well
378 as motile asteroids, ophiuroids and gastropods (Figure 6C-E). Multiple macrouroid fish were in single
379 fields of view (Figure 6C). At the bottom of one escarpment, close to the approximate center of the
380 hydroacoustic water column anomaly, a dense biogenic substrate was seen, which potentially could
381 be bivalves or cnidarians, and might indicate active fluid flow in the sediments (Figure 6E). On the flat,
382 gravelly bottom seafloor areas, partially buried ophiuroids were seen, together with rare occurrences
383 of a decapod lobsterette (Figure 6F). MAPR data recorded during the entire deployment did not reveal
384 any anomaly indicating active fluid flow, i.e. temperature, ORP signal, nephelometer.

385

386



387

388 Figure 6. Potential seep area at Peridotite Location. A) Map showing the transect of PS119/046-1; B)
 389 Arc-parallel scarp with thin sediment layer; C) Densely colonised scarp with suspension feeder
 390 assemblage including comatulid and stalked crinoids, isidid and primnoid octocorals, motile asteroids,
 391 ophiuroids and gastropods, in the soft sediment pennatulid *Umbellula* indet., asteroids and
 392 ophiuroids, and macrourid fish (arrows) present; D) Volcanic outcrop with suspension feeder
 393 assemblage; E) Escarpment with dense biogenic substrate (arrows), potentially bivalves or cnidarians,
 394 on the bottom; F) Gravelly sediment in flat areas with abundant, slightly buried ophiroids and a
 395 decapod lobsterette (arrow).

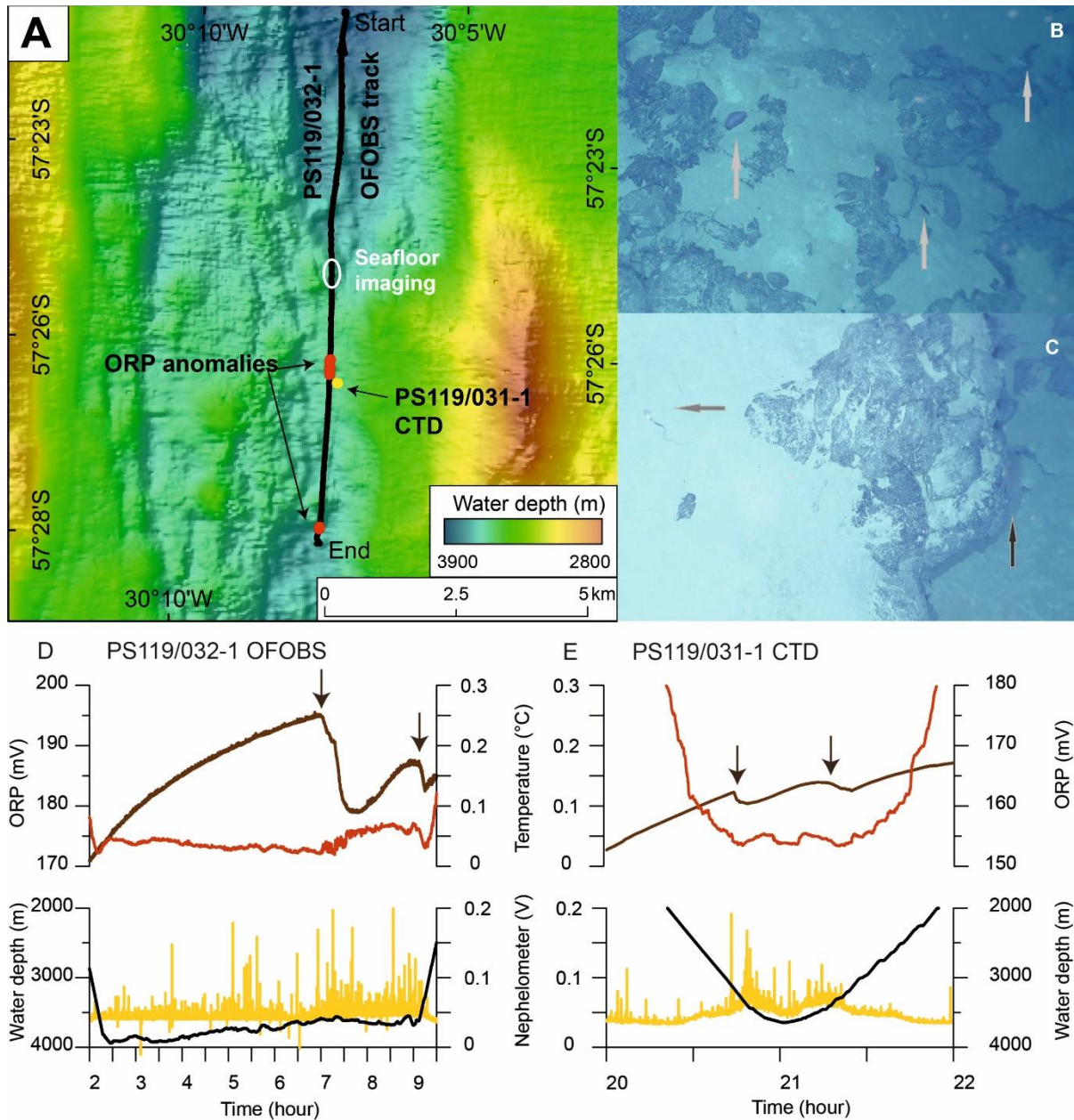
396

397 3.1.8. East Scotia Ridge - Segment E5

398 Based on previously detected water column anomalies indicating hydrothermal activity (German et
 399 al., 2000), the axial rift site at E5 (57°22S 30°07 W, ~3800m) was investigated with MAPRs and
 400 relatively weak anomalies suggested a source of hydrothermal fluids in the area. The MAPR
 401 deployment during PS81/032-1 localised two sites of temperatures anomalies during the micro-

402 bathymetry survey, but the imaging survey missed these sites (Figure 7A, D, E). The area of the imagery
 403 survey showed heavily sedimented pillow lava and escarpments (Figure 7B, C). The sediments
 404 between the pillow lavas were sparsely inhabited by different species of holothurians, stalked crinoids,
 405 ophiuroids and enteropneusts (Figure 7B, C), while few sponges, hydrocorals, ophiuroids and a very
 406 large anemone were seen on the lavas.

407



408
 409 Figure 7. Site of water column anomaly at ESR segment E5. A) Map showing the transect of PS119/032-
 410 1; B) Three different species of holothurians (light grey arrows) on the soft sediment; C) Sedimented
 411 area and pillow lava inhabited by an enteropneust (mid grey arrow) and a very large anemone (black
 412 arrow); D) MAPR detected redox potential, temperature and turbidity anomalies during OFOBS
 413 PS119/032-1; E) MAPR detected redox potential, temperature and turbidity anomalies during CTD
 414 PS119/031-1. OFOBS/CTD profile – black line, redox potential - brown line, temperature - red line,
 415 turbidity yellow line.

416

417 3.2. Megabenthos habitat comparisons between sites

418 For the comparison of megabenthos habitats between sites, the relative percentage abiotic and biotic
 419 substrate cover was assessed based on in-situ images taken from less than 10 m distance (Table 3).
 420 The investigated sites and depths varied in their abiotic substrate and megabenthic faunal traits
 421 (deposit or suspension feeder). The relative biotic substrate cover was low with <0.1% - 4.1%, apart
 422 from the area at the top of the Quest Caldera, where 20.1% of the substrate cover was suspension
 423 feeders, indicating a rich food supply.

424 Table 3. Relative abiotic and biotic substrate cover at the investigated sites

425

Area	Protector Seamounts				Forearc			East Scotia Ridge
	Quest Caldera	Quest Caldera	Quest Caldera	Quest Caldera	off Saunders Island I	off Candlemas Island	Peridotite Location	Segment E5
Location	PS81/268-1&2	PS81/268-2	PS81/268-2	PS81/268-2	PS81/270-1	PS81/273-1	PS119/046-1	PS119/032-1
Depth range	716-744 m / top	outer rim	inner rim	shute	3659-3681 m	3025-3026 m	2500-2313 m	3649-3886 m
No of images	80	77	65	33	46	14	68*	29
Mud	6.9%	43.8%	64.3%	50.3%	49.5%	90.4%	46.8%	52.2%
Sand	-	-	-	-	-	-	-	-
Gravel	-	-	6.8%	8.8%	-	-	13.2%	-
Pebbles	2.2%	26.5%	14.9%	21.9%	24.8%	9.6%	-	-
Cobbles	9.2%	5.6%	3.9%	11.6%	-	-	0.1%	-
Boulders	35.1%	18.0%	3.2%	4.1%	-	-	0.6%	-
Bedrock	-	-	2.4%	-	-	-	31.1%	-
Basalt/pillow lava	-	-	-	-	18.3%	-	-	40.0%
out of sight	25.5%	1.9%	4.1%	1.8%	8.8%	-	5.3%	7.8%
Deposit feeder	0.1%	0.3%	0.2%	0.4%	<0.1%	<0.1%	0.8%	<0.1%
Suspension feeder	20.1%	4.1%	0.4%	1.3%	0.9%	-	2.1%	<0.1%

426

*in-situ images of bedrock areas with dense suspension fauna were taken from >10 m distance

427 **4. Discussion**

428 The RV Polarstern expeditions PS81 and PS119 carried out the first visual investigations of potential
 429 hydrothermally active sites on the Sandwich Plate that had been indicated during previous
 430 explorations as hydroacoustic, light scattering, or sidescan anomalies. Our results were able to
 431 confirm anomalies at the Protector Seamounts and the ESR segment E5 and to present
 432 geomorphology and megafauna information of all investigated sites.

433

434 4.1. Geomorphology and hydrothermal activity

435 The Protector Seamounts form the northernmost part of the South Sandwich Islands volcanic island
 436 arc and the last explosive eruption on the site was noticed in 1962 (Gass et al., 1963, Holdgate, 1963;
 437 Leat et al., 2016). Previous expeditions studied the seafloor bathymetry by single beam and multi-
 438 beam mapping, and dredged samples revealed a dominance of silicic magmatic rocks (Leat et al 2013).
 439 At the southernmost part of the volcanic arc, in the Kemp Caldera, the vents sites are basalt- to basalt
 440 andesite hosted vent chimneys (Cole et al. 2014; Linse et al. 2019; Pape et al., this issue). The in-situ
 441 imagery from the PS81 expedition to the Protector Seamounts revealed pillow lavas, as well as small
 442 chimney structures on the top of the Quest Caldera, but as no physical samples were collected, no
 443 analyses could be done to determine the mineralogy and geochemistry of these chimneys. In the inner
 444 slope of the Adventure Crater, again at the southernmost part of the arc, thin, needle-like chimneys
 445 were seen by towed imagery survey, but no samples were collected (Tyler, 2011). The near-bottom
 446 temperature anomalies of 0.2°C to 1.5° above ambient at Quest Caldera, Protector Shoal and the
 447 unnamed volcano, clearly demonstrate that hydrothermal activity is present in the Protector
 448 Seamounts area. The highest anomalies (2.2°C above ambient) were discovered in the depression on

449 top of the Quest Caldera, where chimney structures were also observed. Temperature anomalies with
450 similar ranges were discovered at the ESR segments E2 and E9, and the southernmost arc Kemp
451 Caldera at sites where active vent fields with hydrothermal venting of 212°C to 383°C were later
452 confirmed (Rogers et al., 2012; Hawkes et al. 2013; Linse et al. 2019). Apart from the chimney
453 structures at Quest Caldera, the Protector Seamounts vent sites have not been localised and no
454 hydrothermal fluid samples have been collected. Therefore, no vent fluid analysis has been done to
455 assess the chemical composition of the end members, especially for iron, (Hawkes et al 2013), which
456 is likely to influence the overlying water column geochemistry and phytoplankton population (Ardyna
457 et al. 2019; Shine et al. 2021).

458 The four sites in the Sandwich Plate forearc can be separated by the background of their previous
459 investigations, based on dredged peridotites off Zavodovski Island (Barker, 1995) and also sidescan
460 anomalies off Candlemas and Saunders islands (Vanneste and Larter, 2002), which could indicate the
461 presence of mud volcanoes. The northern study site off Zavodoski Island, at the Peridotite Location,
462 was based on the record of dredged peridotites (Barker, 1995), which were interpreted as ocean
463 lithosphere modified by metasomatic processes associated with the subduction of the South Sandwich
464 Trench (Pearce et al., 2000; Leat et al., 2016). Research on the mid-Atlantic Ridge Lost City vent field
465 and other locations had created interest in the role of serpentinization of peridotite in generating
466 hydrogen- and methane-rich fluids and supporting chemosynthetic ecosystems (e.g., Charlou et al
467 1998, 2002; Kelley et al., 2001, 2005; Schmidt et al. 2007). Active serpentinization has been studied at
468 the western Pacific Mariana Trench region and revealed a serpentinite-hosted ecosystem (e.g., Ohara
469 et al., 2012; Fryer et al., 2020). The serpentinite mud volcanoes in the Mariana Trench region, Conical
470 and South Chamorro Seamounts, are known to host chemosynthetic bathymodiolin mussels,
471 vesicomid clams, galatheid crabs, actinarians and zoanthid corals (Ohara et al. 2012). These taxa are
472 absent at Lost City, which is known for macrofauna and *Desmophyllum* sp. octocorals (Kelley et al.
473 2005), but bathymodiolin mussels, vesicomid clams and gastropods have been found in a 100 kyr
474 serpentinization-related Ghost City site on the mid-Atlantic Ridge, near the Rainbow vent site (Lartaud
475 et al., 2011). During dive PS119/046-1 no hydrothermal activity, mud volcanoes or chimney structures
476 were discovered, but dense assemblages of alcyonarian corals, crinoids and other suspension feeders
477 were observed at 2330 m to 2500 m depth. This suggests frequent, if not year-round food supply,
478 which in an aphotic zone could be of hydrothermal origin or come via pelagic-benthic coupling from
479 area of high epipelagic primary production. The three study sites off Candlemas and Saunders islands
480 did not reveal hydrothermal mud volcano activity. During dive PS81/270-1 a dense assemblage of
481 white anemones was observed in 3660 m off Saunders Island, with patches of sunken phytodetritus
482 observed nearby.

483 The first indications of hydrothermal activity at the ESR segment E5 were based on water column and
484 sidescan anomalies (German et al., 2000; Livermore et al., 2003, 2006). In 2012, persistent water
485 column anomalies at the site described in German et al. (2000) were confirmed by temperature (0.2°C
486 above ambient) and redox potential anomalies (Tyler, 2013). Equivalent temperature anomalies at the
487 ESR segments E2 and E9 led to the discovery of the active hydrothermal vent fields there (Rogers et
488 al., 2012; Hawkes et al. 2013). During PS119, temperature and redox potential anomalies were
489 confirmed at E5 by MAPRs on OFOBS and CTD deployments, with temperature anomalies of 0.2°C
490 above ambient close to the OFOBS track. Comparing these anomalies with those at E2 and E9, we
491 suggest there is a site of high temperature venting at E5 close to the position investigated during dive
492 PS119/032-1. We recommend that this position should be examined in the future by ROV. The
493 positions of the temperature anomalies were missed by the visual imagery during dive PS119/032-1.
494 The in-situ imagery survey revealed heavily sedimented pillow lavas and basalt rocks, similar to the
495 non-active areas close to the hydrothermal vent fields at E2 and E9 (Linse, Bohrmann, Little and

496 Römer; personal observations during ChEsSO and PS119 expeditions). The basalts analysed previously
497 from E5 were like mid-ocean ridge basalts (MORB), while lavas recovered from E2 and E9 were
498 enriched in Rb, Ba and light rare earth elements compared to MORB (Fretzdorff et al., 2002). The
499 uppermost sections of high-temperature fluid venting chimneys from E2 and E9 were described by
500 James et al. (2014) for their mineralisation and were found to be similar to those found at sediment
501 starved mid-ocean ridge hydrothermal sites.

502

503 4.2. Megabenthic Epifauna

504 Megabenthic epifauna was observed at all the eight investigated sites, from the shallow, 60 m deep
505 top of Protector Shoal to the abyssal, over 3600 m deep ESR segment E5. Additionally, broad, single-
506 bladed macroalgae were observed as a dense cover at the top of Protector Shoal, down to 66 m.
507 Common, large, and single-bladed macroalgae in the Southern Ocean are the brown algae
508 *Himantothallus grandifolius* (A. Gepp & E.S. Gepp) Zinova and the red algae *Sacropeltis antarctica*
509 Hommersand, Hughey, Leister, & P.W. Gabrielson, which are commonly known as dominant benthos
510 cover from 10 m to 40 m, and deeper (Wiencke et al., 2014; Hughey et al., 2020). The megabenthic
511 epifauna observed in the in-situ imagery resembled faunal elements described either from the upper
512 slope of the South Sandwich Islands (Arntz and Brey, 2003; Downie et al., 2021; Hogg et al., 2021), from
513 the Southern Ocean in general (Gutt et al. 2013 and references therein), and from Southern Ocean
514 seamounts (Bowden et al., 2011; Clark and Bowden, 2015). Despite finding evidence for nearby
515 hydrothermal activity (e.g., as temperature anomalies), no recognisable megabenthic Southern Ocean
516 hydrothermal vent taxa were seen, such like yeti crabs, *Sericosura* spp. pycnogonids, peltospirid
517 gastropods, seven-armed star fish, and vesicomylid clams (Marsh et al., 2012; Arango and Linse, 2015;
518 Chen et al., 2015; Mah et al., 2015; Thatje et al., 2015; Linse et al., 2019, 2020). The megafaunal
519 elements recognised on the in-situ imagery included a long-tentacled anemone and decapod spider
520 crabs and lobsterettes.

521 The very large and long-tentacled anemone seen at the ESR segment E5 resembles a member of the
522 deep-sea actinarian family Relicanthidae (Rodriguez et al., 2014). The species *Relicanthus daphneae*
523 (Daly, 2006) has been reported as associated with hydrothermal sites from the Northeast Pacific to
524 the Southern Ocean, including records at the hydrothermal vent sites of the ESR segments E2 and E9
525 (Rogers et al. 2012; Rodriguez et al. 2014).

526 Lithodid crabs, including *Paralomis* indet., were present, sometimes in some density, at all sites on the
527 Protector Seamounts. Records for the South Sandwich Islands list *Paralomis formosa* Henderson,
528 1888, while further *Paralomis* species, *P. anamerae* Macpherson, 1988 and *P. spinosissima* Birstein &
529 Vinogradov, 1972, occur at similar depths at South Georgia (Griffiths et al., 2013).

530 The presence of a decapod lobsterette species and observations of five individuals at 2313-2500 m
531 depth on the Peridotite Location in the South Sandwich Islands northern forearc is a new record of
532 this rarely encountered taxon for the region. The deep-sea Nilenta lobsterette *Thymopsis nilenta*
533 Holthuis, 1974 is known from the south-east of the Falkland Islands and south of South Georgia at
534 1976-3040 m depth (Holthuis, 1974). The depth (2313-2500 m) reported for the lobsterettes from the
535 Peridotite Location is within the known depth range of *T. nilenta* and if this identification could be
536 confirmed the range of *T. nilenta* would be extended 10 degrees longitude to the east of the current
537 known range. Two other lobsterettes are reported from South Georgia. The Patagonian lobsterette
538 *Thymops birsteini* (Zarenkov & Semenov, 1972) and the species *Thymops takedei* Ahyong, Webber &
539 TY Chan, 2012 are known from Southern South America, the Falkland Islands and South Georgia with

540 shallower depth distributions of 122 m to 1400 m and 265 m to 1739 m, respectively (Wahle, 2011;
541 Griffiths et al., 2013). However, without collected specimens the identification of the Peridotite
542 Location lobsterette species is currently unknown.

543 In Antarctic and sub-Antarctic benthic habitats, a common opinion is that suspension feeders
544 dominate in shallower waters while deposit feeders are more abundant at greater depths (Orejas et
545 al., 2000; Gutt et al., 2013; Downie et al. 2021). Suspension feeder assemblages on the high Antarctic
546 continental shelf and at seamounts north of the Ross Sea in 580 m to 600 m depth have been
547 characterised as archaic assemblages based on the dominance of passive, sessile suspension feeders
548 like primnoid and isidid octocorals, sponges, and stalked crinoids (Gili et al., 2006; Bowden et al.,
549 2011). Our study found sessile and mobile suspension feeders to be dominant elements of the
550 epibenthic fauna of the investigated bathyal Sandwich Plate sites, although assemblage composition
551 varied widely between sites and depth. The surveyed abyssal sites in the forearc and ESR in general
552 were inhabited by mobile deposit feeders, like holothurians and burrowing brittle stars. We
553 discovered dense suspension feeder assemblages on the top of the Quest Caldera in ~700 m to 750 m
554 depth and at Peridotite Location in 2300 m to 2500 m depth, with suspension feeders also being
555 present on the slopes of the Protector Shoal volcanoes. These deep dense suspension feeder
556 assemblages occurred in areas with either confirmed (Quest Caldera) or possible (Peridotite Location)
557 hydrothermal activity. We hypothesize that those dense megafaunal assemblages are supported by
558 emissions of hydrothermal fluids in a similar way that Arctic cold seeps support megafauna outside
559 the seeping pockmarks (Åström et al., 2018, 2020).

560 Our investigation of eight sites on the Sandwich Plate has shown that sites with hydrothermal activities
561 are not uncommon, from relatively shallow to abyssal depth. The Sandwich Plate hosts a variety of
562 marine habitats, including seamounts, submarine volcanoes and hydrothermal vents, and the
563 biodiversity assessment of the marine flora and fauna is still incomplete. The geomorphology and
564 localised extents of these habitats will require remotely operated vehicle deployments to collect
565 physical samples for the identification of biological, geological, and chemical origins. Future studies
566 should aim to address the role the hydrothermal habitats play against sunken epipelagic primary
567 production in shaping the regions benthic communities.

568

569 **Declaration of competing interest**

570 The authors declare that they have no known competing financial interests or personal relationships
571 that could have appeared to influence the work reported in this paper.

572

573 **CRediT authorship contribution statement**

574 **Katrin Linse:** Conceptualization, Validation, Formal analysis, Investigation, Data curation, Writing –
575 original draft, Writing review & editing, Visualization. **Miriam Römer:** Methodology, Investigation,
576 Data curation, Writing review & editing. **Crispin T.S. Little:** Investigation, Writing review & editing.
577 **Yann Marcon:** Methodology, Software, Writing review & editing. **Gerhard Bohrmann:** Writing review
578 & editing, Project administration, Funding acquisition.

579

580 Acknowledgements

581 We grateful to the support by the masters and crews of RV Polarstern expeditions ANT XXIX-4 and
582 PS119. The research group ‘‘Biosciences, Deep Sea Ecology and Technology’’ (Dr. Autun Purser) of the
583 Alfred Wegener Institute for Polar and Marine Research, Bremerhaven, Germany, is thanked for
584 providing the seafloor observatory systems (OFOS & OFOBS), respectively. Sharon Walker from NOAA
585 Seattle is acknowledged for providing and supporting the MAPRs via her MARUM collaboration. We
586 thank Eberhard Kopsiske and Paul Wintersteller for their technical support to the OFOS/OFOBS and TV-
587 sled systems, Ricarda Dziadek for the MTL support, and Stefanie Gaide, Victoria K rztzinger, Nontje
588 R cker, Yiting Tseng, Ines Vejzovic and Tingting Wu for their participation in the observation shifts.
589 Martin Collins and two anonymous reviewers are thanked for their constructive comments which
590 improved a previous version.

591 The field work for this study, including participation of GB, YM and MR, was supported by the Deutsche
592 Forschungsgemeinschaft (DFG) in the framework of the priority program ‘Antarctic Research with
593 comparative investigations in Arctic ice areas’ by a grant to BO 1049/19, through the DFG-Research
594 Center/Cluster of Excellence ‘‘The Ocean in the Earth System’’ and by the BMBF via Projekttr ger J lich
595 (03G0880A). Cruise PS119 was funded by the German Federal Ministry of Education and Research
596 (grant no. 03G0880A) and by the German Research Foundation (Deutsche Forschungsgemeinschaft,
597 DFG) through the Cluster of Excellence ‘The Ocean Floor – Earth’s Uncharted Interface’ (EXC-2077 –
598 project number 390741603) at MARUM–Center for Marine and Environmental Sciences, University of
599 Bremen. KL is part of the British Antarctic Survey Polar Science for Planet Earth Programme (NC
600 Science), funded by The Natural Environment Research Council (NERC). CTSL acknowledges travel
601 funds from the Earth Surface Sciences Institute, University of Leeds that helped him take part in the
602 Polarstern cruises.

603 Studies in the East Scotia Sea were undertaken under permits WAP/2013/027 (PS81) and permit RAP
604 2018/064(PS119) issued by the South Georgia and South Sandwich Government.

605

606 Data management

607 PS81 and PS119 data, including images, videos and hydroacoustic recordings are stored in the World
608 Data Center PANGAEA Data Publisher for Earth & Environmental Science (www.pangaea.de) with a
609 secured access.

610

611 References

612 Arango, C.P., Linse, K., 2015. New *Sericosura* (Pycnogonida: Ammotheidae) from deep-sea
613 hydrothermal vents in the Southern Ocean. *Zootaxa* 3995, 37-50. doi: 10.11646/zootaxa.3995.1.5.

614 Ardyna, M., Lacour, L., Sergi, S. et al., 2019. Hydrothermal vents trigger massive phytoplankton blooms
615 in the Southern Ocean. *Nat. Commun.* 10, 2451. doi:10.1038/s41467-019-09973-6

616 Arntz, W.E; Brey, T., 2003. Expedition ANTARKTIS XIX/5 (LAMPOS) of RV Polarstern in 2002. *Ber.*
617 *Polarforsch. Meeresforsch.* 462, 1-120.

618 Arntz, W.E., Lovrich, G.A., Thatje, S., 2004a. The Antarctic-Magellan connection: links and frontiers at
619 southern high latitudes. Summary review. *Sci. Marina* 69 (suppl 2), 3-5.

620 Arntz, W.E., Thatje, S., Gerdes, D., Gili, J.-M., Gutt, J., Jacob, U., Montiel, A., Orejas, C., Teixido, N.,
621 2004b. The Antarctic-Magellan connection: macrobenthos ecology on the shelf and upper slope, a
622 progress report. *Sci. Marina* 69 (suppl 2), 237-269.

623 Åström, E.K.L., Carroll, M.L., Ambrose JR., W.G., Sen, A., Silyakova, A., Carroll, J., 2018. Methane cold
624 seeps as biological oases in the high-Arctic deep sea. *Limnol. Oceanogr.* 63, S209-S231.
625 doi.org/10.1002/lno.10732

626 Åström, E.K.L., Sen, A., Carroll, M.L., Carroll, J., 2020. Cold Seeps in a Warming Arctic: Insights for
627 Benthic Ecology, *Front. Mar. Sci.*, 10.3389/fmars.2020.00244.

628 Barker, P.F., 1978. The South Sandwich Islands: III. Petrology of the volcanic rocks. *Brit. Ant Surv. Sci.*
629 Rep. 93, 1-34.

630 Barker, P.F., 1995. Tectonic framework of the East Scotia Sea. In Taylor B., ed. *Backarc basins: tectonics*
631 *and magmatism*. New York: Plenum Press, pp. 281-314.

632 Bohrmann, G., Chin, C., Petersen, S., Sahling, H., Schwarz-Schampera, U., Greinert, J., Lammers, S.,
633 Rehder, G., Daehlmann, A., Wallmann, K., Dijkstra, S., Schenke, H.-W., 1999. Hydrothermal activity at
634 Hook Ridge in the Central Bransfield Basin, Antarctica. *Geo. Mar. Lett.* 18, 277-284.

635 Bohrmann, G., with contributions of the participants, 2013. The expedition of the research vessel
636 "Polarstern" to the Antarctic in 2013 (ANT-XXIX/4), *Ber. Polarforsch. Meeresforsch.* 668, 1-169. doi:
637 10.2312/BzPM_0668_2013

638 Bohrmann, G., with contributions of the participants, 2019. The Expedition PS119 of the Research
639 Vessel POLARSTERN to the Eastern Scotia Sea in 2019, *Ber. Polarforsch. Meeresforsch.* 736, 1-236.
640 [doi:10.2312/BzPM_0736_2019](https://doi.org/10.2312/BzPM_0736_2019)

641 Bongiovanni, C., Stewart, H.A., Jamieson, A.J., 2021. High-resolution multibeam sonar bathymetry of
642 the deepest place in each ocean. *Geosci. Data J.* 00, 1-16. <https://doi.org/10.1002/gdj3.122>

643 Bowden, D.A., Schiaparelli, S., Clark, M.R., Rickard, G.J., 2011. A lost world? Archaic crinoid-dominated
644 assemblages on an Antarctic seamount. *Deep-Sea Res. II* 58, 119–127. doi:10.1016/j.dsr2.2010.09.006

645 Brandt, A., De Broyer, C., Gooday, A.J., Hilbig, B., Thomson, M.R., 2004. Introduction to ANDEEP
646 (ANTarctic benthic DEEP-sea biodiversity: colonization history and recent community patterns)—a
647 tribute to Howard L. Sanders. *Deep Sea Res. Pt II.* 51(14-16), 1457-1465.

648 Brandt, A., Gooday, A.J., Brandao, S.N., Brix, S., Brökeland, W., Cedhagen, T., Choudhury, M., Cornelius,
649 N., Danis, B., De Mesel, I., Diaz, R.J., Gillan, D.C., Ebbe, B., Howe, J., Janussen, D., Kaiser, S., Linse, K.,
650 Malyutina, M., Nunes Brandao, S., Pawlowski, J., Raupach, M., Vanreusel, A., 2007. The Southern
651 Ocean deep sea: first insights into biodiversity and biogeography. *Nature* 447,307-311.

652 Brasier, M.J., Wiklund, H., Neal, L., Jeffreys, R., Linse, K., Ruhl, H., Glover, A.G., 2016. DNA barcoding
653 uncovers cryptic diversity in 50% of deep-sea Antarctic polychaetes. *R. Soc. Open Sci.* 3, 160432.

654 Charlou, J.L., Fouquet, Y., Bougault, H., Donval, J.P., Etoubleau, J., Jean-Baptiste, P., Dapoigny, A.,
655 Appriou, P., Rona, P.A., 1998. Intense CH₄ plumes generated by serpentinization of ultramafic rocks
656 at the intersection of the 15°20'N fracture zone and the Mid-Atlantic Ridge. *Geochim. Cosmochim.*
657 *Acta* 62, 2323–2333. [https://doi.org/10.1016/S0016-7037\(98\)00138-0](https://doi.org/10.1016/S0016-7037(98)00138-0)

658 Charlou, J.L., Donval, J.P., Fouquet, Y., Jean-Baptiste, P., Holm, N., 2002. Geochemistry of high H₂ and
659 CH₄ vent fluids issuing from ultramafic rocks at the Rainbow hydrothermal field (36°14'N, MAR).
660 Chem. Geol. 191, 345–359. [https://doi.org/10.1016/S0009-2541\(02\)00134-1](https://doi.org/10.1016/S0009-2541(02)00134-1)

661 Chen, C., Linse, K., Roterman, C.N., Copley, J.T., Rogers, A.D., 2015. A new Genus of large hydrothermal
662 vent-endemic gastropod (Neomphalina: Peltospiridae) with two new species showing evidence of
663 recent demographic expansion. Zool. J. Linn. Soc. 175, 319-335.

664 Clark, M.R., Bowden, D.A., 2015. Seamount biodiversity: high variability both within and between
665 seamounts in the Ross Sea region of Antarctica. Hydrobiol. 761, 161-180. doi: 10.1007/s1070-015-
666 2327-9

667 Clubbe, C., 2018. South Georgia & the South Sandwich Islands Marine Protected Area 5-year Review
668 Report to the Government of South Georgia and the South Sandwich Islands. Available online at:
669 [http://www.gov.gs/docsarchive/Environment/Marine%20Protected%20Area/SGSSI_5year_MPA_Review_Summary_Report_to_GSGSSI_\(Nov%202018\).pdf](http://www.gov.gs/docsarchive/Environment/Marine%20Protected%20Area/SGSSI_5year_MPA_Review_Summary_Report_to_GSGSSI_(Nov%202018).pdf)
670

671 Cole, C.S., James, R.H., Connelly, D.P., Hathorne, E.C., 2014. Rare earth elements as indicators of
672 hydrothermal processes within the East Scotia subduction zone system. Geochim. Cosmochim. Acta
673 140, 20-38. doi:10.1016/j.gca.2014.05.018.

674 Downie, A.-L., Vieira, R.P., Hogg, O.T., Darby, C., 2021. Distribution of Vulnerable Marine Ecosystems
675 at the South Sandwich Islands: Results from the Blue Belt Discovery Expedition 99 Deep-Water Camera
676 Surveys. Front. Mar. Sci. 8, 662285. doi: 10.3389/fmars.2021.662285

677 Fretzdorff, S., Livermore, R.A., Devey, C.W., Leat, P.T., Stoffers, P., 2002. Petrogenesis of the Back-arc
678 East Scotia Ridge, South Atlantic Ocean. J. Pet. 43, 1435-1467.

679 Fryer, P., Wheat, C.G., Williams, T., et al., 2020. Mariana serpentinite mud volcanism exhumes
680 subducted seamount materials: implications for the origin of life. Phil. Trans. R. Soc. A 378, 20180425.
681 Doi:10.1098/rsta.2018.0425

682 Gass, I.G., Harris, P.G., Holdgate, M.W., 1963. Pumice eruption in the area of the South Sandwich
683 Islands. Geol. Mag. 100, 321–330.

684 German, C.R., Livermore, R.A., Baker, E.T., Bruguier, N.I., Connelly, D.P., Cunningham, A.P., Morris, P.,
685 Rouse, I.P., Statham, P.J., Tyler, P.A., 2000. Hydrothermal plumes above the East Scotia Ridge: an
686 isolated high-latitude back-arc spreading centre. Earth. Planet. Sci. Lett. 184, 241-250.

687 Gili, J.-M., Arntz, W.E., Palanques, A., Orejas, C., Clarke, A.C., Dayton, P.A., Isla, E., Teixido, N., Rosssi,
688 S., Lopez-Gonzales, P.J., 2006. A unique assemblage of epibenthic sessile suspension feeders with
689 archaic features in the high-Antarctic. Deep-Sea Res. II 53, 1029–1052.

690 Grant, R.A., Linse, K., 2009. Barcoding Antarctic biodiversity: current status and the CAML initiative.
691 Polar Biol. 32, 1629-1637.

692 Griffiths, H.J., Waller, C.L., 2016. The first comprehensive description of the biodiversity and
693 biogeography of Antarctic and Sub-Antarctic intertidal communities. J. Biogeogr 43, 1141-1155.

694 Griffiths, H.J., Whittle, R.J., Roberts, S.J., Belchier, M., Linse, K., 2013. Antarctic Crabs: Invasion or
695 Endurance? PLoS One 5(8), e11683. doi:10.1371/journal.pone.0011683

696 Gutt, J., Griffiths, H.J., Jones, C.D., 2013. Circumpolar overview and spatial heterogeneity of Antarctic
697 macrobenthic communities. Mar. Biodiv. 43, 481-487. doi: 10.1007/s1 2526-013-0152-9

698 Hawkes, J. A., Connelly, D.P., Gledhill, M., Achterberg, E.P., 2013. The stabilisation and transportation
699 of dissolved iron from high temperature hydrothermal vent systems, *Earth Planet. Sci. Lett.*, 375, 280–
700 290.

701 Hawkes, J.A., Connelly, D.P., Rijkenberg, M.J.A., Achterberg, E.P., 2014. The importance of shallow
702 hydrothermal island arc systems in ocean biogeochemistry. *Geophys. Res. Lett.* 41, 942-947,
703 doi:10.1002/2013gl058817.

704 Hogg, O. T., Barnes, D. K. A., and Griffiths, H. J., 2011. Highly diverse, poorly studied and uniquely
705 threatened by climate change: an assessment of marine biodiversity on South Georgia’s continental
706 shelf. *PLoS One* 6, e19795. doi: 10. 1371/journal.pone.0019795

707 Hogg, O.T., Huvenne, V.A.I., Griffiths, H.J., Linse, K., 2016. On the ecological relevance of landscape
708 mapping and its application in the spatial planning of very large marine protected areas. *Sci. Total*
709 *Environ.* <https://doi.org/10.1016/j.scitotenv.2018.01.009>

710 Holdgate, M.W., 1963. Observations in the South Sandwich Islands, 1962. *Polar Rec.* 11 (73), 394–405.

711 Holthuis, L.B., 1974. Biological results of the University of Miami Deep-Sea Expeditions. 106. The
712 lobsters of the superfamily Nephropidea of the Atlantic Ocean (Crustacea: Decapoda). *Bull. Mar. Sci.*
713 24(4), 723-884.

714 Horton, T., Marsh, L., Bett, B.J., Gates, A.R., Jones, D.O., Benoist, N., Pfeifer, S., Simon-Lledó, E.,
715 Durden, J.M., Vandepitte, L., Appeltans, W., 2021. Recommendations for the standardisation of open
716 taxonomic nomenclature for image-based identifications. *Front. Mar. Sci.* 8, 620702.
717 <https://doi.org/10.3389/fmars.2021.620702>

718 Hughley, J.R., Leister, G.L., Gabrielson, P.W., Hommersand, M.H., 2020. *Sarcopeltis* gen. nov.
719 (Gigartinaceae, Rhodophyta), with *S. skottsbergii* comb. nov. from southern South America and *S.*
720 *antarctica* sp. nov. from the Antarctic Peninsula. *Phytotaxa* 468, 14. doi:10.11646/phytotaxa.468.1.4.

721 James, R.H., Green, D.R.H., Stock, M.J., Alker, B.J., Banerjee, N.R., Cole, C., German, C.R., Huvenne,
722 V.A.I., Powell, A.M., Connelly, D.P., 2014. Composition of hydrothermal fluids and mineralogy of
723 associated chimney material on the East Scotia Ridge back-arc spreading centre. *Geochim.*
724 *Cosmochim. Acta* 139, 47-71. doi:10.1016/j.gca.2014.04.024.

725 Jamieson, J.A., Stewart, H.A., Weston, J.N.J., Bongiovanni, C., 2021. Hadal fauna of the South Sandwich
726 Trench, Southern Ocean: Baited camera survey from the Five Deeps Expedition. *Deep Sea Res. Pt II*
727 194. 104987. <https://doi.org/10.1016/j.dsr2.2021.104987>. Kelley, D.S., Karson, J., Blackman, D., et al.,
728 2001. An off-axis hydrothermal vent field near the Mid-Atlantic Ridge at 30°N. *Nature* 412, 145-149.
729 <https://doi.org/10.1038/35084000>

730 Kelley, D.S., Karson, J.A., Früh-Green, G.L., et al., 2005. A serpentinite-hosted ecosystem: the Lost City
731 hydrothermal field. *Science* 307.1428–1434. doi: 10.1126/science.1102556

732 Maljutina, M., 2004. Russian deep-sea investigations of Antarctic fauna. *Deep Sea Res. Pt II.* 51(14-
733 16), 1551-1570. <https://doi.org/10.1016/j.dsr2.2004.07.012>

734 Lartaud, F., Little, C.T.S., de Rafelis, M., Bayon, G., Dymont, J., Ildefonse, B., Gressier, V., Fouquet, Y.,
735 Gaill, F. and Le Bris, N. 2011. Fossil evidence for serpentinitization fluids fueling chemosynthetic
736 assemblages. *Proc. Nat. Acad. Sci.* 108, 7698–7703.

737 Larter, R.D., Vanneste, L.E., Morris, P., Smythe, D.K., 2003. Structure and tectonic evolution of the
738 South Sandwich arc, in: Larter, R., Leat, P.T. (Eds.), *Intra-Oceanic Subduction Systems: Tectonic and*
739 *Magmatic Processes*. Geological Society, London, Special Publications, pp. 255-284.

740 Leat, P.T., Larter, R.D., Millar, I.L., 2007. Silicic magmas of Protector Shoal, South Sandwich arc:
741 indicators of generation of primitive continental crust in an island arc. *Geol. Mag.* 144, 179–190.

742 Leat, P.T., Day, S.J., Tate, A.J., Martin, T.J., Owen, M.J., Tappin, D.R., 2013. Volcanic evolution of the
743 South Sandwich volcanic arc, South Atlantic, from multibeam bathymetry. *JVGR* 265, 60-77.
744 doi:10.1016/j.jvolgeores.2013.08.013.

745 Leat, P.T., Fretwell, P.T., Tate, A.J., Larter, R.D., Martin, T.J., Smellie, J.L., Jokat, W., Bohrmann, G.,
746 2016. Bathymetry and geological setting of the South Sandwich Islands volcanic arc. *Ant. Sci.* 28, 293-
747 303, doi:10.1017/S0954102016000043.

748 Leat, P.T., Livermore, R.A., Millar, I.L., Pearce, J.A., 2000. Magma supply in back-arc spreading centre
749 segment E2, East Scotia Ridge. *J. Pet.* 41, 845-866. doi:10.1093/petrology/41.6.845.

750 Leat, P.T., Pearce, J.A., Barker, P.F., Millar, I.L., Barry, T.L., Larter, R.D., 2004. Magma genesis and
751 mantle flow at a subducting slab edge: the South Sandwich arc-basin system. *Earth. Planet. Sci. Lett.*
752 227, 17-35. doi:10.1016/j.epsl.2004.08.016.

753 Linse, K., Copley, J.T., Connelly, D.P., Larter, R.D., Pearce, D.A., Polunin, N.V.C., Rogers, A.D., Chen, C.,
754 Clarke, A., Glover, A.G., Graham, A.G.C., Huvenne, V.A.I., Marsh, L., Reid, W.D.K., Roterman, C.N.,
755 Sweeting, C.J., Zwirgmaier, K., Tyler, P.A., 2019. Fauna of the Kemp Caldera and its upper bathyal
756 hydrothermal vents (South Sandwich Arc, Antarctica). *R. Soc. Open Sci.* 6, 191501.
757 doi:10.1098/rsos.191501.

758 Linse, K., Sigwart, J.D., Chen, C., Krylova, E.M., 2020. Ecophysiology and ecological limits of
759 symbiotrophic vesicomid bivalves (Pliocardiinae) in in the Southern Ocean. *Polar Biol.* 43, 1423-1437.
760 doi:10.1007/s00300-020-02717-z.

761 Livermore, R., 2003. Back-arc spreading and mantle flow in the East Scotia Sea. In: Larter, R.D., Leat,
762 P.T. (Eds.), *Intra-Oceanic Subduction Systems: Tectonic and Magmatic Processes*. Geological Society,
763 London Special Publications, 219, pp. 315–331.

764 Livermore, R. 2006. The East Scotia Sea: Mantle to Microbe. *Geophys. Monograph Ser.* 166, 243-261.

765 Mah, C., Linse, K., Copley, J.T., Marsh, L., Rogers, A., Clague, D., Foltz, D., 2015. Description of a New
766 Family, including New Genera and Species of deep-sea Forcipulatacea (Asteroidea), the first known
767 sea star from Hydrothermal Vent Settings. *Zool. J. Linn. Soc.* 174,93-113.

768 Marsh, L., Copley, J.T., Huvenne, V.A.I., Linse, K., Reid, W.D.K., Rogers, A., Sweeting, C.J., Tyler, P.,
769 2012. Microdistribution of faunal assemblages at deep-sea hydrothermal vents in the Southern Ocean
770 *PLoS One* 7, e48348. doi:10.1371/journal.pone.0048348

771 Meyer, K.S., Bergmann, M., Soltwedel, T., 2013. Interannual variation in the epibenthic megafauna at
772 the shallowest station of the HAUSGARTEN observatory (79° N, 6° E). *Biogeosciences* 10, 3479–3492.
773 <https://doi.org/10.5194/bg-10-3479-2013>.

774 Ohara, Y., Reagan, M.K., Fujikura, K., Watanabe, H., Michibayashi, K., Ishii, T., Stern, R.J., Pujana, I.,
775 Martinez, F., Girard, G., Ribeiro, J., Brounce, M., Komori, N., Kino, M., 2012. A serpentinite-hosted
776 ecosystem in the Southern Mariana Forearc. *Proc. Nat. Acad. Sci.* 109 (8), 2831-2835. doi:
777 10.1073/pnas.1112005109

778 Orejas, C., Gili, J.M., Arntz, W.E., Ros, J.D., López, P.J., Teixidó, N., Filipe, P., 2000. Benthic suspension
779 feeders, key players in Antarctic marine ecosystems? *Contrib. Sci.* 1, 299-311.

780 Park, S.-H., Langmuir, C.H., Sims K.W.W., Blichert-Toft, J., Kim, S.-S., Scott, S.R., Lin, J., Choi, H., Yang,
781 Y.-S., Michael, P.J., 2021. An isotopically distinct Zealandia-Antarctic mantle domain in the Southern
782 Ocean. *Nat. Geosci.* 12, 206-214.

783 Pearce, J.A., Barker, P.F., Edwards, S.J., Parkinson, I.J., Leat, P.T., 2000. Geochemistry and tectonic
784 significance of peridotites from the South Sandwich arc-basin system, South Atlantic. *Contrib. Mineral.*
785 *Petrol.*, 139, 36-53.

786 Pfender, M., Villinger, H., 2002. Miniaturized data loggers for deep sea sediment temperature gradient
787 measurements, *Mar. Geol.* 186, 557-570. doi.org/10.1016/S0025-3227(02)00213-X.

788 Purser, A., Marcon, Y., Dreutter, S., Hoge, U., Sablotny, B., Hehemann, L., Lemburg, J., Dorschel, B.,
789 Biebow, H., Boetius, A., 2019. Ocean Floor Observation and Bathymetry System (OFOBS): A New
790 Towed Camera/Sonar System for Deep-Sea Habitat Surveys. *IEEE J. Ocean. Eng.* 44, 87-99.

791 Reid, W.D.K., Sweeting, C.J., Wigham, B.D., Zwirgmaier, K., Hawkes, J.A., McGill, R.A.R., Linse, K.,
792 Polunin, N.V.C., 2013. Spatial differences in East Scotia Ridge hydrothermal vent food webs: influences
793 of chemistry, microbiology and predation on trophodynamics. *PLoS One* 9 (6) e65553.

794 Rauschert, M., Arntz, W. (2015). Antarctic Macrobenthos: A field guide of the invertebrates living at
795 the Antarctic seafloor). Arntz & Rauschert Selbstverlag. ISBN 978-3-00-049890-9

796 Riuz, M.B., Taverna, A., Servetto, N., Sahade, R., Held, C., 2020. Hidden diversity in Antarctica:
797 Molecular and morphological evidence of two different species within one of the most conspicuous
798 ascidian species. *Ecol. Evol.* 10.8127-8143.

799 Rodriguez, E., Barbeitos, M.S., Brugler, M.R., Crowley, L.M., Grajales, A., et al., 2014. Hidden among
800 Sea Anemones: The First Comprehensive Phylogenetic Reconstruction of the Order Actiniaria
801 (Cnidaria, Anthozoa, Hexacorallia) Reveals a Novel Group of Hexacorals. *PLoS One* 9(5), e96998.
802 doi:10.1371/journal.pone.

803 Rogers, A.D., Linse, K., 2014. Chemosynthetic communities. In: De Broyer et al. (eds) *The CAML/ SCAR*
804 *MarBIN Biogeographic Atlas of the Southern Ocean*. Chapter 5.30, 240-244.

805 Rogers, A.D., Tyler, P.A., Connelly, D.P., Copley, J.T., James, R., Larter, R.D., Linse, K., Mills, R.A., et al.,
806 2012. The discovery of new deep-sea hydrothermal vent communities in the Southern Ocean and
807 implications for biogeography. *PLoS Biol.* 10(1): e1001234. doi:10.1371/journal.pbio.1001234.

808 Schine, C.M.S., Alderkamp, AC., van Dijken, G. Gerringa, L.J.A., Sergi, S., Laan, P., van Haren, H., van de
809 Poll, W.H., Arrigo, K.R., 2021. Massive Southern Ocean phytoplankton bloom fed by iron of possible
810 hydrothermal origin. *Nat. Commun.* 12, 1211. <https://doi.org/10.1038/s41467-021-21339-5>

811 Smellie, J.L., Morris, P., Leat, P.T., Turner, D.B., Houghton, D., 1998. Submarine caldera and other
812 volcanic observations in Southern Thule, South Sandwich Islands. *Antarct. Sci.* 10, 171-172.

813 Schmidt, K., Koschinsky, A., Garbe-Schönberg, D., de Carvalho, L.M., Seifert, R., 2007. Geochemistry of
814 hydrothermal fluids from the ultramafic-hosted Logatchev hydrothermal field, 15°N on the Mid-
815 Atlantic Ridge: Temporal and spatial investigation. *Chem. Geol.* 242, 1-21.
816 <https://doi.org/10.1016/j.chemgeo.2007.01.023>

- 817 Spiess, V., Breitzke, M., 1990. Das Parasound-Sedimentecholotsystem - Funktionsweise,
818 Anwendungsbeispiele and digitale Datenerfassung, Jahrestagung der Deutschen Geologischen
819 Gesellschaft, Bremen.
- 820 Stewart, H.A., Jamieson, A.J., 2019. The five deeps: The location and depth of the deepest place in
821 each of the world's oceans. *Earth-Sci. Rev.* 197, 102896. doi.org/10.1016/j.earscirev.2019.102896
- 822 Talley, L.D., Pickard, G.L., Emery, W.J., Swift, J.H., 2011. The Southern Ocean. In: Talley et al (eds)
823 Descriptive Physical Oceanography. Academic Press, Chapter 13: pp 437-471.
824 Doi.org/10/1016/C2009-0-24322-4
- 825 Thatje, S., Marsh, L., Roterman, C.N., Mavrigordate, M.N., Linse, K., 2015. Adaptations to
826 hydrothermal vent life in *Kiwa tyleri*, a new species of yeti crab from the East Scotia Ridge, Antarctica.
827 PLoS One 10(6): e0127621.doi:10.1371/journal.pone.017621
- 828 Trathan, P. N., Collins, M. A., Grant, S. M., Belchier, M., Barnes, D. K. A., Brown, J., et al. 2014. The
829 South Georgia and South Sandwich Islands MPA: protecting a biodiverse oceanic island chain situated
830 in the flow of the Antarctic Circumpolar Current. *Adv. Mar. Biol.* 69, 15–77.
- 831 Tyler, P.A., et al., 2011. Cruise Report RRS James Cook Cruise JC55. 13 January to 22 February 2011.
832 Bransfield Strait, the East Scotia Ridge and the Kemp Seamount Calderas - Cruise 3 of the NERC
833 Consortium Grant 'Chemosynthetically-driven ecosystems in the Southern Ocean: Ecology and
834 Biogeography' (ChEsSo). https://www.bodc.ac.uk/resources/inventories/cruise_inventory/report/
- 835 Tyler, P.A., et al., 2013. Cruise Report RRS James Cook Cruise JC80. 2 December to 30 December 2013.
836 Bransfield Strait, the East Scotia Ridge and the Kemp Seamount Calderas - Cruise 4 of the NERC
837 Consortium Grant 'Chemosynthetically-driven ecosystems in the Southern Ocean: Ecology and
838 Biogeography' (ChEsSo). https://www.bodc.ac.uk/resources/inventories/cruise_inventory/report/
- 839 Vanneste, L.E., Larter, R., 2002. Sediment subduction, subduction erosion, and strain regime in the
840 northern South Sandwich forearc. *J. Geophys. Res.* 107, 2149. doi:10.1029/2001JB000396
- 841 Van Wyk de Vries, M., Bingham, R.G. & Andrew S. Hein, A.S., 2017. A new volcanic province: an
842 inventory of subglacial volcanoes in West Antarctica. In: Exploration of Subsurface Antarctica:
843 Uncovering Past Changes and Modern Processes. Geological Society, London, Special Publications,
844 461. doi: 10.1144/SP461.7
- 845 Wahle, R., 2011. *Thymopsis nilenta*. The IUCN Red List of Threatened Species 2011:
846 e.T170024A6711317. <https://dx.doi.org/10.2305/IUCN.UK.2011-1.RLTS.T170024A6711317.en>.
847 Downloaded on 27 August 2021.
- 848 Walker, S.L., Baker, E.T., Resing, J.A., Nakamura, K., McLain, P.D., 2007. A new tool for detecting
849 hydrothermal plumes: an ORP Sensor for the PMEL MAPR. *Eos Trans, AGU88* (52). Fall Meet. Suppl.,
850 Abstract V21D-0753.
- 851 Wiencke, C., Amsler, C.D., Clayton, M.N., 2014. Macroalgae. In De Broyer, C., Koubbi, P., Griffiths, H.J.,
852 Raymond, B., D'Udekem D'Acoz, C., Van de Putter, A.P., Dans, B., David, B., Grant, S., Gutt, J., Held, C.
853 Hosie, G., Huettmann, F., Post, A., Robert-Coudert, Y., eds. Biogeographic Atlas of the Southern Ocean.
854 Cambridge, UK: Scientific Committee on Antarctic Research, 66-73.